Open access • Posted Content • DOI:10.1101/2021.08.13.456288

Responses of Escherichia coli and Listeria monocytogenes to ozone treatment on non-host tomato: Efficacy of intervention and evidence of induced acclimation

de los Reyes, Shu, Singh, Karampudi ...+3 more authors

Institutions: Texas Tech University

Published on: 15 Aug 2021 - bioRxiv (Cold Spring Harbor Laboratory)

Topics: Listeria monocytogenes

Responses of *Escherichia coli* and *Listeria monocytogenes* to ozone treatment on non-host tomato: Efficacy of intervention and evidence of induced acclimation

Xiaomei Shu[1,2□], Manavi Singh[1□], Naga Bhushana Rao Karampudi[1□], David F. Bridges[3□], Ai Kitazumi[1], Vivian C. H. Wu[1,3*], Benildo G. De los Reyes[1*]

[1]Department of Plant and Soil Science, Texas Tech University, Lubbock, TX 79409, USA

[2]Center for Biotechnology and Genomics, Texas Tech University, Lubbock, TX 79409, USA

[3]USDA-ARS, Western Regional Research Center, Produce Safety and Microbiology Research, Albany, CA 94710, USA

[*]Correspondence: benildo.reyes@ttu.edu, vivian.wu@usda.gov

[□]These authors contributed equally to this work.

Xiaomei Shu: xiaomei.shu@ttu.edu

Manavi Singh: manavi.singh@ttu.edu

Naga Bhushana Rao Karampudi: bhushan.karampudi@ttu.edu

Ai Kitazumi: ai.kitazumi@ttu.edu

David F. Bridges: David.Bridges@usda.gov

Short Title: *Responses of Escherichia coli and Listeria monocytogenes to ozone treatment on non-host tomato*

Abstract

Because of the continuous rise of foodborne illnesses caused by the consumption of raw fruits and vegetables, effective post-harvest anti-microbial strategies are needed. This study evaluated the dose × time effects on the anti-microbial action of ozone (O_3) gas against the Gram-negative *Escherichia coli* O157:H7 and Gram-positive *Listeria monocytogenes,* which are common contaminants in fresh produce. The study on non-host tomato environment correlated the dose × time aspects of xenobiosis by examining the correlation between bacterial survival in terms of log-reduction and defense responses at the level of gene expression. In *E. coli*, low (1 µg O_3/g of fruit) and moderate (2 µg O_3/g of fruit) doses caused insignificant reduction in survival, while high dose (3 µg/g of fruit) caused significant reduction in survival in a time-dependent manner. In *L. monocytogenes*, moderate dose caused significant reduction even with short-duration exposure. Distinct responses to O_3 xenobiosis between *E. coli* and *L. monocytogenes* are likely related to differences in membrane and cytoplasmic structure and components.

Transcriptome profiling by RNA-Seq showed that primary defenses in *E. coli* were attenuated after exposure to a low dose, while the responses at moderate dose were characterized by massive upregulation of pathogenesis and stress-related genes, which implied the activation of defense responses. More genes were downregulated during the first hour at high dose, with a large number of such genes getting significantly upregulated after 2 hr and 3 hr. This trend suggests that prolonged exposure led to potential adaptation. In contrast, massive downregulation of genes was observed in *L. monocytogenes* regardless of dose and exposure duration, implying a mechanism of defense distinct from that of *E. coli*. The nature of bacterial responses revealed by

this study should guide the selection of xenobiotic agents for eliminating bacterial contamination on fresh produce without overlooking the potential risks of adaptation.

Keywords

Escherichia coli O157:H7, *Listeria monocytogenes*, *Solanum lycopersicum*, ozone gas, RNA-Seq, transcriptional regulatory networks, adaptation

Introduction

Perennial outbreaks of foodborne illnesses due to changes in pathogen population dynamics have an astonishing impact to human health [1-4]. In the United States alone, it was estimated that more than 30% of food-related deaths are due to the combined effects of only two bacterial pathogens, *i.e., Listeria monocytogenes* (28%) and *Escherichia coli* O157:H7 (3%) [5], both of which have been blamed for the more recent outbreaks on fresh vegetables including tomato (*Solanum lycopersicum* L.) [6, 7]. These pathogenic bacteria can survive under a wide range of environmental conditions and often contaminate their non-host plants at several developmental stages, and along the pre-harvest and post-harvest production pipelines through multiple routes [8, 9]. For instance, even a brief exposure of wounded tomato fruits to *E. coli* O157:H7 can provide an effective inoculum for widespread contamination during subsequent post-harvest handling and processing [10, 11].

Strategies including on-farm hygiene, decontamination by washing, film coating, prophage induction, and the use of chemical interventions that involve sodium hypochlorite (NaClO), sodium chlorite ($NaClO_2$), acidified $NaClO_2$, acidified sodium benzoate (NaB), or peracetic acid (PAA) are common means for post-harvest control of bacterial contamination on fresh tomatoes and other types of vegetables [12-14]. Ozone gas (O_3) has been widely used decontaminating agent for eliminating *E. coli* O157:H7 and *L. monocytogenes* on various types of surfaces, including seeds, fresh fruits, as well as other organic and inorganic substrates such as milk and water [15-18]. However, the long-term impacts of such chemical intervention to potential acclimation, adaptation, and selection caused by chronic exposure to selective doses are often overlooked. For example, viable but non-culturable state of *E. coli* O157:H7 induced by exposure to various types of environmental stresses could contribute to adaptation [19]. The

93 effects of environmental stresses including acid induced adaptation has also been shown to cause
94 an acclimation effect in *L. monocytogenes* [20]. To address these concerns, comprehensive
95 understanding of the potential consequences of sub-optimal, optimal, and supra-optimal doses
96 and duration of exposure to chemical intervention is important in order to prevent future
97 outbreaks caused by the proliferation of resistant strains triggered by acclimation to strong
98 selective pressures [8].

99 Human-pathogenic bacteria respond to environmentally induced perturbations by
100 employing a variety of defense or avoidance mechanisms [21, 22]. Bacterial defenses could be
101 stimulated initially by different types of environmental factors, and such stimulation could
102 further lead to a 'priming effect' that builds resistance to subsequent episodes of stress [23, 24].
103 For example, studies have shown that heat stress effectively primes *E. coli* O157 to develop
104 resistance to subsequent exposure to acidic environments [25]. While surviving on non-host
105 environments, such as the surfaces of fresh fruits and vegetables, bacterial cells are subjected to
106 intense stress pressure, which could lead to acquired tolerance to other stresses or persistence as
107 a viable inocula for much longer periods until they are revitalized in a suitable host environment
108 [26]. Acquired resistance to environmental stresses could eventually promote anti-microbial
109 resistance (AMR) through defense mechanisms that are effective against a broad range of
110 chemical intervention agents. These AMR mechanisms also enable microorganisms to resist the
111 anti-microbial effects of chemical agents, and such resistance has been suggested to be a major
112 cause of perennial outbreaks in the food industry. For example, disinfectant-injured and
113 genetically distinct sub-populations of *E. coli* believed to have originated from the widespread
114 use of chlorine-based agents and O_3 have been identified in water. There are also indications that

these treatments trigger the proliferation of genetically distinct sub-populations that arise from the injurious but non-lethal effects of such chemical agents [27].

In our previous analysis of the transcriptional responses of *E. coli* O157:H7 to gaseous chlorine dioxide (ClO_2) on non-host tomato environment, we uncovered characteristic gene expression signatures which indicated that optimal dose x time interaction causes an effective reduction of bacterial viability with evidence of injury and killing. However, gene expression signatures also indicated that supra-optimal dose x time effects could trigger resistance through acclimation or adaptation. Patterns in ClO_2-mediated changes in gene expression revealed that longer exposure even under a dosage as low as 1 µg could effectively trigger new bursts of independent defense mechanisms on the surviving sub-populations of bacteria after the effective killing phase. These trends pointed to the occurrence of adaptation and selection in residual sub-populations surviving on the surface of non-host tomato [26]. Guided by these findings, we examined the effects of another commonly used chemical intervention agent, ozone (O_3) gas on the Gram-negative *E. coli* O157:H7 and Gram-positive *L. monocytogenes* in context of the potential consequences of dose x time effects not only on the intervention efficacy but also on potential AMR on a common non-host environment, *i.e.,* fresh tomatoes. We discuss here the biological significance of the transcriptional networks associated with potential xenobiotic effects of O_3 on *E. coli* and *L. monocytogenes*, and the implications of dose x time interaction to optimal and supra-optimal effects.

Methods and Methods

Microbial inocula

E. coli O157:H7 (ATCC 35150) and *L. monocytogenes* (ATCC 19115) were from the permanent cultures of the U.S. Department of Agriculture-Agricultural Research Service, Western Regional Research Center's Pathogenic Microbiology Laboratory. Working cultures used throughout the study were maintained on tryptic soy agar (TSA) a 4°C and were inoculated from frozen stocks maintained at -80 °C in 25% glycerol broth. Prior to experimentation, the bacterial strains were cultured overnight at 37°C in tryptic soy broth (TSB), centrifuged at 5000xG for 15 min, re-suspended in 10 ml 0.1% peptone water, centrifuged for another 15 min and re-suspended in 12 ml 0.1% peptone water.

Samples of fresh tomato without post-harvest processing were obtained from Windset Farms, California. Tomato fruits without visual damage or mold growth were washed with water and, surface sterilized with 70% ethanol, and dried in the hood. Aliquots of 250 µl of bacterial suspension were inoculated on the surface of each tomato fruit, followed by air drying for a few hours. Inoculated fruits were placed in sterile plastic bags and incubated overnight at 4°C. Twelve tomato fruits were weighed (2.0 ± 0.1 kg) and used for each O_3 treatment. Three replicates consisting of twelve tomato fruits in each replicate were included for each treatment. Tomato fruits were treated with 1 µg per g tomato fruits (low dose), 2 µg per g tomato fruits (moderate dose) or 3 µg per g tomato fruits (high dose) of O_3 as previously described [8, 28].

Regrowth assay on *E. coli* and *L. monocytogenes*

After 1 hr, 2 hr and 3 hr of O_3 treatment, each tomato fruit that was inoculated with either *E. coli* or *L. monocytogenes* was rinsed with 10 ml 0.1% peptone water for 1 min for serial

dilution (10^{-1} to 10^{-5}) and plating using MacConkey Sorbital Agar supplemented with 0.05 mg/l Cefixime and 2.5 mg/L PotassiumTellurite (CT-SMAC) for *E. coli* or Polymyxin acriflavine lithium chloride ceftazidime aesculin mannitol (PALCAM) agar supplemented with 10 mg/l polymyxin B, 20 mg/l ceftazidime, and 5 mg/l acriflavine for *L. monocytogenes*. Both media were layered with a thin layer of TSA to aid in the recovery of sub-lethally injured cells. Samples were incubated overnight at 37°C and bacterial growth assay (log CFU/g) was determined by comparing O_3-treated samples with the control according to standard procedures [8].

RNA-Seq library construction, sequencing, and data processing

Bacterial RNA samples were isolated from each combination of dose (1 µg, 2 µg, 3 µg) and exposure duration (1 hr, 2 hr, 3 hr) in *E. coli* and *L. monocytogenes* using a Quick-RNA™ Fungal/Bacterial RNA Microprep kit (Zymo Research) according to the manufacturer's instructions. For each sample, three replicates were used to construct three RNA-Seq libraries, which were then pooled and sequenced twice at 900x depth per library. Sequencing was performed on the Illumina HiSeq-3000 at 150-bp paired-end reads at the Genomics Core Facility, Oklahoma Medical Research Foundation, Norman, OK, USA.

Raw sequence reads from RNA-Seq were processed according to standard protocols [29]. Raw data were preprocessed with Cutadapt (v1.9.1) to remove adapters and low-quality sequences to generate paired 100-bp reads [30]. Subsequently, data with at least 16 million pairs per library were mapped using Edge-Pro (version v1.3.1) to account for polycistronic gene organization [31]. Reference *E. coli* O157:H7 str. Sakai genome (Genbank: GCA_000008865.2, NCBI: ASM886v2) and *L. monocytogenes* EGD-e (Genbank:

183 GCA_000196035.1, NCBI: ASM19603v1) were used for mapping based on high map rates
184 (~98%) of control sample and availability of pathway annotation in KEGG [32].
185
186 **Propensity transformation and transcriptome analysis**
187 Relative changes in gene expression expressed as Propensity Scores (PS) were
188 established from the standard RPKM-based expression data using two batches of sequences for
189 control (t_0), 1 hr (t_1), 2 hr (t_2) and 3 hr (t_3) for all three doses of O_3. Average RPKM were
190 transformed using the Propensity Transformation methodology that was optimized from the ClO_2
191 study on *E. coli* [66] based on the following equation:

192 $$\mathrm{Pti} = \ln\left(\frac{\frac{Ti}{\sum_{j=t_0}^{t_3} T_{ij}}}{\frac{\sum_{i=1}^{5192} T_j}{\sum_{j=t_0}^{t_3}\sum_{i=1}^{5192} T_{ij}}}\right)$$

193 Where, Pt_i=Propensity transformation of RPKM value of transcript *i*
194 T_i= RPKM value of transcript *i*
195 *j*=Variable that iterates over datasets of t_0=control, t_1= 1 hr, t_2 = 2 hr and t_3 = 3 hr
196 *i*=Variable that iterates over the total number of transcript-encoding loci
197
198 Missing data in the dataset was considered as NULL and its transformed value was
199 considered 0. The PS data from each library were assumed to form a normal distribution ranging
200 between -n to +n, which were further fragmented into 20 quartiles based on the propensity
201 scores. Quartile cuts resulted in 250 transcripts per quartile in all the datasets. Two quartiles per
202 dataset representing the transcripts with the lowest and the highest propensity scores were
203 subsequently selected for transcriptional regulatory network analysis, resulting 500 transcript-

encoding loci per dataset (Additional file 3: Table S2). Two-way hierarchical clustering analysis with both RPKM values and PS values was performed using JMP, 11 (SAS Institute Inc., Cary, NC, USA).

Genetic network modeling

A subset of normalized RPKM values were selected to calculate the standard Pearson Correlation Coefficient (PCC) using the Python Pandas library. The dataset was derived from the PS values without log transformation containing only positive values. The PCC for one versus all transcripts were calculated using this subset of normalized RPKM that resulted in a diagonally symmetrical matrix of 5129 × 5129 coefficients in which the diagonal values represent the PCC of every transcript locus with itself.

Transcript-encoding gene loci for network modeling were selected via two filtration steps: first using the PS followed by PCC. PS-based selection is as explained above using the quartile cuts that resulted in a group of transcript-encoding loci and their highly correlated co-expression partners were selected using the PCC values. The second step of transcript selection was based on PCC with cut-off of 0.9999 for filtration of positively and negatively correlated transcript loci. This selection represented the most likely O_3-affected gene loci that were significant according to PS and their highly correlated co-upregulated, co-downregulated, or inversely co-expressed loci from the primary selection.

Results

Dose and time effects of O_3 on *Escherichia coli* and *Listeria monocytogenes*

To understand the importance of dose × time dynamics on the xenobiotic action of O_3 on foodborne bacterial pathogens, we compared the effects of chemical treatments on fresh tomato fruits between the Gram-negative *E. coli* O157:H7 and Gram-positive *L. monocytogenes* under a non-host environment provided by fresh tomatoes. We investigated the efficacy of bacterial killing by examining regrowth on fresh media using the washings from inoculated tomato fruits after different durations of treatment at different doses. Exposure to a low dose caused only mild effects on *E. coli* based on minimal reduction in viability and partial reduction ($P > 0.05$) in growth rates over time (Fig. 1). However, upon exposure to a moderate dose, there was a partial killing effect on *E. coli* after the first hour, followed by a slight increase in growth after the second and third hours ($P > 0.05$; Fig. 1A). The slight increases observed during the second and third hours indicate a 'shock' effect, which appeared to be short-lived based on apparent recovery after prolonged exposure. The mean bacterial cell recovery for *E. coli* O157:H7 at a high dose was low after the first hour ($P > 0.05$). Further reduction in bacterial survival continued on with longer exposure through the second and third hours ($P < 0.05$; Fig. 1A).

Similar to the trends observed in *E. coli*, the effects of low dose (1 µg) and short duration (1 hr) exposure on the viability of *L. monocytogenes* on non-host tomato was very mild (Fig. 1B; $P > 0.05$). However, moderate and high doses caused a significant reduction in survival as indicated by the decline in bacterial counts even after short (1 hr) exposure. The effects of moderate and high doses continued through the second and third hours, although the magnitude during prolonged exposure appeared to be relatively mild ($P < 0.05$; Fig. 1B). In summary, the bacterial regrowth assays for *E. coli* and *L. monocytogenes* from the O_3-treated fresh tomatoes

250 across different doses and exposure time indicate that the impact of O_3 xenobiosis was generally
251 mild and appeared to have different levels of efficacy in the Gram-negative *E. coli* and Gram-
252 positive *L. monocytogenes.* While the dose effects were similar between the two species of
253 bacteria, the effect of exposure time appeared to vary. These trends appeared to indicate that the
254 response mechanisms of the Gram-negative *E. coli* and Gram-positive *L. monocytogenes* are
255 quite distinct.

256 Determining the optimal dose and exposure time that could induce effective killing of
257 bacterial contaminants on the surface of a labile, non-host fresh produce such as tomato is a
258 critical aspect of effective chemical intervention. Optimal dose and exposure time that maintain
259 the overall physical and biochemical properties of the fresh produce are of prime importance. In
260 the case of O_3, a dose of 3 μg per gram of tomato fruits for up to 3 hr of treatment is the highest
261 possible strength that can be applied without drastic impacts on sensory attributes and quality.
262 Our earlier studies indicated that the highest efficacy of ClO_2 xenobiosis requires a moderate
263 dose and long exposure, which was not observed in the O_3 assays for both *E. coli* and *L.*
264 *monocytogenes* [33]. Therefore, based on the results of bacterial regrowth assays across dose and
265 time combinations, O_3 appeared to be less effective than ClO_2 in reducing bacterial
266 contamination on fresh tomatoes. O_3 causes only mild killing effects on both *E. coli* and *L.*
267 *monocytogenes* even at the highest dose and time exposure within the threshold level that
268 maintains the overall sensory quality of tomato fruits. Compared to the overall effects of ClO_2,
269 given that only partial killing could be achieved at best with O_3, we hypothesize that its
270 utilization as a chemical agent for intervention has a higher likelihood of inducing adaptation and
271 acclimation effects than ClO_2.
272

Transcriptomic changes in response to O_3 xenobiosis in *E. coli* and *L. monocytogenes*

We profiled the transcriptomes of *E. coli* and *L. monocytogenes* in the context of dose × time responses as a means to understand the nature of defenses and how those defenses are compromised when O_3 xenobiosis triggered partial killing effects [30]. RPKM expression values across the temporal RNA-Seq datasets were normalized and transformed to Propensity Scores (PS). Pearson Correlation Coefficient (PCC) was further applied to PS in order to establish the significance of differentially expressed genes [30]. Based on the scatter plots of the global O_3-response transcriptomes, similar patterns of transcriptional changes were evident over time during exposure of *E. coli* to low and moderate doses of O_3 (Fig. 2A; Additional File 1: Fig. S). The responses triggered by low and moderate doses were characterized by the general downregulation of gene expression, which was particularly more pronounced during the second hour and continued through the third hour. On top of the general patterns of downregulation, there appears to be a certain subset genes that were upregulated during the second hour.

The global O_3-response transcriptome of *E. coli* under a high dose is characterized by even more significant downregulation of gene expression, which was evident as early as during the first hour. The apparent perturbation appeared to suggest that higher doses are much more effective, although the xenobiotic effects are not quite evident during short duration (first hour) exposure as indicated by the growth reduction data ($P > 0.05$; Fig. 1A; Fig. 2A). Strikingly, as O_3 treatment is prolonged through the third hour, the response transcriptome appeared to show indications of recovery from the initially perturbed state as indicated by the significant reversal of downregulated genes towards upregulation (Fig. 2A). These signs of recovery correlated with the results of the regrowth assay, suggesting that reduction in growth due to xenobiosis was substantially attenuated during the second and third hours ($P < 0.05$; Fig. 1A). These trends

296 further suggest a gradual recovery of the surviving bacterial sub-populations, which are likely
297 consequences of potential adaptation due to chronic effects.

298 In stark contrast, the global O_3-response transcriptome of *L. monocytogenes* under a low
299 dose appeared to be more perturbed as indicated by the widespread downregulation of gene
300 expression during the entire period (first to third hours) of treatment (Fig. 2B). This trend seemed
301 to be contradictory to the patterns in regrowth assay when reduction in bacterial regrowth was
302 not very apparent (Fig. 1B). At moderate to high doses, the global transcriptomes were
303 apparently perturbed, as indicated by the massive downregulation of gene expression throughout
304 the entire three-hour duration of exposure. This trend was consistent with a significant reduction
305 in bacterial viability ($P < 0.05$) as indicated by the regrowth assay (Fig. 1B).

306 The RNA-Seq data matrix revealed that the expression of a total of 2,488 genes in *E. coli*
307 (48.5% of total protein-coding genes) and 1,801 genes in *L. monocytogenes* (63.5% of total
308 protein-coding genes) were altered during the three-hour treatment period, as evident from
309 different patterns of downregulation and upregulation across time (Fig. 2C and 2D; Additional
310 file 2: Table S1). In *E. coli,* a total of 73, 964, and 9 genes were uniquely upregulated in response
311 to low dose during the first, second and third hours, respectively. In *L. monocytogenes*, there
312 were 22, 8 and 1,233 uniquely upregulated genes in response to low dose during the first, second
313 and third hours, respectively. These temporal changes in gene expression indicate a gradual
314 response to a low dose of O_3 that appeared to peak with longer periods of exposure. The
315 significant spikes in the number of upregulated genes during the third hour indicate that defenses
316 are progressively induced with longer exposure, which is consistent with the overall patterns in
317 the regrowth assay where log-reduction in bacterial growth was only mild even with a longer
318 duration of exposure (Fig. 1C).

At a moderate dose, a total of 210, 570, and 118 genes in *E. coli* were uniquely upregulated during the first, second, and third hours, respectively. Moderate dose also caused the downregulation of 604, 286, and 86 genes in during the first, second, and third hours, respectively (Fig. 2C). These opposite patterns in the upregulation and downregulation of gene expression during prolonged exposure suggest that defense responses are gradually stabilized over time under a non-lethal dose of O_3. Gradual stabilization of defense responses implies that perturbation is diminished or repaired over time under non-lethal dose, which is consistent with the resurgence of bacterial growth based on the higher proportions of viable cells recovered during the third hour of treatment as indicated by the regrowth assay (Fig. 1A).

During the first hour of exposure to a high dose, 392 genes were upregulated, and 194 genes were downregulated in *E. coli* (Fig. 2C). Notably, there was a drastic decline in the number of upregulated genes from 392 to only 16 during the second hour, which was accompanied by a spike in the total number of downregulated genes from 194 to 1,165 (Fig. 2C). During the third hour, a total of 689 genes were upregulated, and 148 genes were downregulated (Fig. 2C). The large proportion of downregulated genes during the second hour suggests that severe perturbation hence killing effects have occurred, consistent with the log-reduction data (Fig. 1A). However, the spike in the number of upregulated genes during the third hour suggests significant recovery, likely as a result of acclimation during prolonged exposure (Fig. 1A).

Exposure of *L. monocytogenes* to a low dose caused the upregulation of 124, 124, and 236 genes during the first, second, and third hours of treatment, respectively, and downregulation of 145, 145, and 120 genes during the first, second, and third hours, respectively (Fig. 1D). These changes imply that at low dosage, defense responses in *L. monocytogenes* are not fully active unless the bacterial population is subjected to prolonged exposure. Under moderate dose,

342 which caused significant reduction in bacterial regrowth (Fig. 1B), a total of 121, 112, and 124
343 genes were uniquely upregulated, during the first, second, and third hours, respectively, while
344 162, 162, and 277 genes were uniquely downregulated during the first, second, and third hours,
345 respectively. These trends in gene activation and repression across time are indicative of
346 attenuated defense response, particularly during longer exposure (Fig. 2D). Further increase to a
347 high dose caused the upregulation of 66, 83, and 73 genes during the first, second, and third
348 hours, respectively, and downregulation of 68, 100, and 70 genes during the first, second, and
349 third hours, respectively (Fig. 2D). During exposure of *L. monocytogenes* to a high dose, much
350 larger number of differentially expressed genes overlapped at during short, medium and longer
351 duration, which are suggestive of potential adaptation.
352
353 **Chronic exposure causes a new burst of defenses**
354 Exposure of *E. coli* to a low dose of O_3 was accompanied by upregulation of 815 genes
355 during the second hour, while the same subset of genes drastically shifted to downregulation
356 during the third hour (Additional file 2: Table S1). Under a moderate dose, a subset of 346 genes
357 that were downregulated during the first hour shifted to upregulation during the second hour.
358 These drastic shifts in gene expression indicate that a new burst of defense responses may have
359 been triggered likely due to the intense selection pressure associated with longer exposure even
360 at moderate dose. We also observed that a subset of 423 genes that were downregulated during
361 the second hour at high dose drastically shifted to upregulation during the third hour. This
362 suggests that potential acclimation of the surviving sub-populations during prolonged exposure
363 may have likely occurred.

364 Under low dose, few genes in *L. monocytogenes* that were upregulated during the second
365 and third hours shifted to downregulation with longer exposure to moderate (2 µg) and high (3
366 µg) doses. This subset of genes is enriched with regulatory functions that are important for
367 defense mechanisms, including the Rrf2 family protein gene (LMOf2365_2331), NifU family
368 protein (LMOf2365_2371), FUR family transcriptional regulator (LMOf2365_1986), and GlnR
369 family transcriptional regulator (LMOf2365_1316) (Additional file 2: Table S1).
370 In both *E. coli* and *L. monocytogenes,* the peculiar gene expression signatures associated
371 with dose x time response were enriched with functions associated with pathogenicity, response
372 to stress, regulation of cell division, cell motility, amino acid and protein metabolism,
373 transcription and RNA processing, transport, carbohydrate metabolism, nucleotide metabolism,
374 and genetic recombination (Fig. 3; Additional file 2: Table S1). In *E. coli*, a large proportion of
375 genes associated with pathogenesis and stress response were progressively downregulated from
376 the first to the second hour under low dose. A significant proportion of these genes shifted to
377 upregulation during the third hour (Fig. 3A). With a further increase in dose to moderate, genes
378 associated with pathogenesis and stress response were either upregulated or downregulated
379 across time (Fig. 3A). However, under a high dose, a much larger proportion of pathogenesis and
380 defense response genes were significantly downregulated during the first and third hours but
381 upregulated during the second hour. These trends are suggestive of a new burst of expression of
382 defense-associated genes, an event that is likely independent of the responses that occurred
383 during the first hour (Fig. 3A). In contrast, genes associated with pathogenicity, stress response,
384 cell division, and cell motility were upregulated in *L. monocytogenes* during exposure to low,
385 moderate, and high doses across time (Fig. 3B).

386 Two-way hierarchical clustering of Propensity Scores (PS) and RPKM values revealed
387 20 distinct clades representing different patterns of co-expression across the *E. coli* and *L.*
388 *monocytogenes* transcriptomes (Fig. 4; Additional file 2: Table S1). In *E. coli*, clustering of PS
389 according to dose x time regimes showed that expression signatures in 1 μg O_3 × 1 hr treatment
390 regime were more similar to the signatures of 3 μg O_3 × 1 hr treatment regime, while the
391 expression signatures of 1 μg O_3 × 2 hr regime clustered with the signatures of 3 μg O_3 × 3 hr
392 regime (Fig. 4A). The expression signatures based on RPKM data indicate that the profiles of 1
393 μg O_3 × 1 hr and 1 μg O_3 × 2 hr treatment regimes formed a single clade, while the profiles of 1
394 μg O_3 × 3 hr and 3 μg O_3 × 3 hr treatment regimes formed a separate clade (Fig. 4A). In *L.*
395 *monocytogenes*, the gene expression signatures of 1 μg O_3 × 1 hr, 1 μg O_3 × 2hr, 1 μg O_3 × 3 hr,
396 and 2 μg O_3 × 3 hr treatment regimes were more similar, characterized by more significant
397 downregulation. Expression signatures of the other treatment regimes formed a separate clade
398 characterized by significant upregulation (Fig. 4B). These trends indicate that defense responses
399 were attenuated at a low dosage but much enhanced at a higher dosage.
400
401 **Effects of O_3 on genes associated with pathogenicity, stress response, and defenses**
402 T3SS represents an important class of genes involved in bacterial pathogenicity, encoding
403 multi-protein complex channels that inject effectors to promote bacterial attachment to the host
404 [34]. The transcriptomes of *E. coli* revealed a total of 29 T3SS-encoding genes with altered
405 expression, particularly in response to high dose (Fig. 5A; Additional file 2: Table S1). Of these
406 genes, 17 were upregulated in the 3 μg O_3 × 1 hr treatment regime, and 10 were upregulated in
407 the 3 μg O_3 × 3 hr treatment regime. An additional 21 T3SS-encoding genes were downregulated
408 in the 3 μg O_3 × 2 hr treatment regime (Fig. 5A; Additional file 2: Table S1). Differential

409 expression of these T3SS genes indicates that xenobiotic effects at high dose compromised
410 pathogenicity, particularly with moderately extended time up to 2 hours. During the third hour,
411 there is an indication of a rebound of pathogenicity, likely as a consequence of prolonged
412 exposure.

413 In *L. monocytogenes*, expression of 14 genes that belong to the general class of T2SS-
414 pathogenesis proteins were affected by exposure to O_3. Of these, five (5) genes encoding ATP-
415 binding protein (LMOf2365_1360), comEC/Rec2 family protein (LMOf2365_1501), general
416 secretion pathway protein E (LMOf2365_1364), and general secretion pathway protein F
417 (LMOf2365_1363) were downregulated in 1 µg O_3 × 1 hr treatment regime, and another
418 helicase-encoding gene (LMOf2365_2486) was stably downregulated throughout the three-hour
419 period of O_3 treatment (Fig. 5B; Additional file 2: Table S1).

420 A total 18 genes involved in biofilm formation were affected by O_3 treatments in *E. coli*
421 (Fig. 5A; Additional file 2: Table S1). Under low dose, several of these biofilm-associated genes
422 were upregulated during the first and second hours, and then subsequently downregulated during
423 the third hour. At a higher dose, another subset of biofilm-associated genes that were initially
424 downregulated during the first hour were subsequently upregulated through the second and third
425 hours. With further increase to a high dose, another subset of biofilm-associated genes was
426 upregulated during the first and third hours but downregulated during the second hour. These
427 expression signatures imply that the process of biofilm formation was attenuated during brief
428 exposure to O_3 regardless of the dosage, but the same process appeared to be enhanced with
429 longer exposure to much higher doses with longer exposure. In contrast to the large effects of O_3
430 on biofilm-associated genes in *E. coli*, only four (4) biofilm-associated genes were affected in *L.*
431 *monocytogenes*, including those encoding diguanylate cyclase (LMOf2365_1940,

LMOf2365_1941), which were downregulated during the first hour at low dose (Fig. 5B; Additional file 2: Table S1).

As a critical component of cell-to-cell communication in bacteria, quorum sensing facilitates the monitoring of cell population density, detection of xenobiotic molecules, and translation of extracellular signals to intercellular processes and downstream gene expression [35]. The response transcriptomes of *E. coli* and *L. monocytogenes* included 31 and 15 quorum sensing-associated genes, respectively, that were significantly affected by O_3 (Fig. 5; Additional file 2: Table S1). In *E. coli*, these genes were downregulated during short (1 hr) and long (3 hr) duration exposure to low dose. At a moderate dose, these genes were downregulated during the first and third hours but upregulated during the second hour. With further increase to a high dose, these genes were upregulated during the first hour, downregulated during the second hour, and subsequently dramatically upregulated during the third hour. In *L. monocytogenes*, two (2) quorum sensing genes were upregulated during the first and second hour at a low dose, and another gene was downregulated during the third hour. However, at moderate and high doses, quorum sensing genes exhibited different patterns of upregulation or downregulation across time, suggesting that a comprehensive defense system is triggered *L. monocytogenes* under higher strength of O_3 xenobiosis.

The two-component system plays an important role in bacterial responses to environmental changes, which is critical in maintaining pathogenicity and fitness under adverse conditions [36]. The transcriptome data revealed a total of 41 and 21 genes associated two-component systems that were affected by O_3 in *E. coli* and *L. monocytogenes,* respectively (Fig. 5; Additional file 2: Table S1). Of the 41 affected genes in *E. coli*, 24 were significantly upregulated at low dose during the second hour, while 21 genes were downregulated during the

455 third hour. At higher dose, several two-component system-associated genes were upregulated
456 during the first and third hours but were attenuated during the second hour. As mentioned in the
457 previous section, transient upregulation of a large number of genes at high dose with longer
458 exposure are likely indicators of acclimation possibly due to chronic effects (Fig. 1). In *L.*
459 *monocytogenes*, most of the genes associated with the two-component system were
460 downregulated, with only a few being upregulated, particularly under high dose, suggesting that
461 O_3 has a more significant impact in suppressing the two-component system in *L. monocytogenes*
462 than *E. coli.*

463 In addition to the effects on T3SS/T2SS, biofilm, quorum-sensing, and two-component
464 associated genes, O_3 also had significant effects on other classes of stress-related genes in both
465 *E. coli* and *L. monocytogenes*. For instance, in *E. coli*, several genes encoding SOS response
466 proteins, thiol:disulfide interchange protein, putative tellurium resistance protein, and
467 chemotaxis-associated proteins were affected at different time-points (Additional file 2: Table
468 S1). In addition, six heat shock protein genes (HSPs) were upregulated during the third hour
469 under low dose but downregulated during the first hour under moderate dose. With a further
470 increase to a high dose, genes that function in the regulation of energy metabolism [37] as well
471 as phosphotransferase system HPr enzyme (ECs4354) were downregulated during the second
472 hour but upregulated during the third hour.

473 In *L. monocytogenes,* genes associated with stress response were under high dose,
474 including an amidophosphoribosyltransferase (LMOf2365_1793), 2-oxoisovalerate
475 dehydrogenase E1 subunit beta (LMOf2365_1390), transketolase (LMOf2365_2640), and ABC
476 transporter ATP-binding protein/permease (LMOf2365_2732). Other types of stress-related
477 genes such as ribose-5-phosphate isomerase B (LMOf2365_2654), heat shock protein GrpE

(LMOf2365_1493), and heat-inducible transcription repressor (LMOf2365_1494) were upregulated. Few genes involved in antibiotic biosynthesis were also affected by O_3 in both *E. coli* and *L. monocytogenes*, indicating that O_3 elicit responses similar to the defense mechanisms against antibiosis.

Certain genes involved in the regulation of bacterial transcription such as *sigma-E factor* are key players in biofilm formation and pathogenicity [38-40]. The transcriptome data revealed that O_3 had an effect on the expression of certain transcriptional regulatory proteins associated with biofilm formation and pathogenicity in both *E. coli* and *L. monocytogenes.* For example, in *E. coli*, the *sigma-E regulatory protein* gene (ECs3436) was upregulated during the first hour and then subsequently downregulated during the second hour under moderate dose (Additional file 2: Table S1). Potential suppression of biofilm-associated genes appeared to be supported by concomitant downregulation of translational activities as suggested by the downregulation of 12 ribosome-associated genes. In *L. monocytogenes*, the *transcription termination factor Rho* (LMOf2365_2523) was downregulated during the entire period (first to third hour) under high dose.

Transcriptional networks associated with bacterial responses to O_3

We selected the genes that were most significantly affected by O_3 in a dose x time dependent manner in both *E. coli* and *L. monocytogenes.* These included the genes with the lowest and highest PS across the three doses used in the experiments. A cut-off of 0.9999 was further applied to filter out both positively and negatively correlated changes in gene expression. At this stringency of filtration, 1,588, 1,276 and 1,405 genes in *E. coli* represent the most statistically significant changes in expression during the first, second, and third hours,

501 respectively. Similarly, 1,221, 1,312 and 1,119 genes in *L. monocytogenes* represent the most
502 statistically significant changes during the first, second and third hours, respectively. These
503 groups of genes were used to model the transcriptional co-expression networks to understand the
504 effects of O_3 xenobiosis on the global response mechanisms of each bacterial species (Additional
505 file 3: Table S2). Pearson Correlation Coefficients (PCC) identified 674, 781, and 934 genes that
506 were differentially expressed in *E. coli* under low (1 µg), moderate (2 µg), and high (3 µg) doses
507 $_3$, respectively (Additional file 2: Table S1; Additional file 3: Table S2). Similarly, PCC
508 identified 876, 591, and 736 genes that were differentially expressed in *L. monocytogenes* under
509 low, moderate and high doses, respectively (Additional file 2: Table S1; Additional file 3: Table
510 S2).

511 Under low dose, the transcriptional network of *E. coli* during the first hour is
512 characterized by few small clusters of co-expressed genes at the center of the global network
513 (Fig. 6A). During the second hour, large clusters of genes appeared to be coordinately regulated
514 in either positive (co-upregulation) or negative (co-downregulation) direction without an
515 apparent connection to a central hub or core regulator. During the third hour, larger clusters of
516 co-expressed genes started forming a discernible connection to a central hub or core regulator.
517 Under moderate and high doses, the networks included few small reorganized secondary clusters
518 during the entire three hours of exposure (Fig. 6A). This trend appears to suggest that high doses
519 possibly led to acclimation, based on the reduced magnitude of gene expression changes relevant
520 to the defense. These results indicate that *E. coli* responds to low and high doses in very different
521 ways, similar to the dose-dependent responses reported earlier for ClO_2 [33].

522 The O_3-response networks of *L. monocytogenes* appeared to be quite distinct from those
523 of *E. coli*, supporting our hypothesis that *L. monocytogenes* is more sensitive to O_3 as indicated

524 by the regrowth assays (Fig. 1A). Under low dose O_3, a small cluster of co-expressed genes was
525 evident at the center of the global network during the first and second hours but not during the
526 third hour (Fig. 6B). With further increase to a moderate dose, small clusters began to form at the
527 center of the global network particularly during the first and second hour, which appeared to
528 have resulted to a much larger cluster during the third hour (Fig. 6B). Under high dose, large
529 clusters were evident during the entire three-hour duration of exposure (Fig. 6B).
530

531 **Discussion**

532 **Acclimation of bacterial pathogens to non-host intermediate vectors**

533 Gram-positive bacteria have cell walls made of a thick layer of peptidoglycan, while the
534 cell walls of Gram-negative bacteria are composed of a thin layer of peptidoglycan and an outer
535 membrane that is absent in Gram-positive bacteria. Gram-negative and Gram-positive bacteria
536 have employed different molecular strategies to cope with the environmental changes and to
537 interact with their hosts [41]. The Gram-negative *E. coli* and Gram-positive *L. monocytogenes*
538 are among the most dangerous bacterial pathogens notorious for their ubiquitous occurrence
539 across a broad range of environments. Their persistent nature and strong virulence have been
540 attributed to their toxin production capacities and low infectious doses, causing high mortality
541 rates in both humans and animals [3, 7, 42-46]. For instance, illnesses caused by the foodborne
542 Shiga toxin-producing *E. coli* O157 (STEC) can be life-threatening, with a very low dose (20
543 and 700 cells) in contaminated fresh produce capable of causing major outbreaks [47]. In recent
544 times, *E. coli* serotype O157:H7 has been the major cause of outbreaks by contaminating fresh
545 vegetables during the post-harvest processing pipeline [7]. *E. coli* O157:H7 is flexible in terms of
546 its adaptability to extreme fluctuations in the environment, due in part to its short life cycle and

547 highly efficient genetic regulatory machineries that confer highly flexible defense systems [48,
548 49]. Harsh environmental conditions are largely responsible for triggering viable but non-
549 culturable (VBNC) populations of bacteria, which provide an effective inoculum when
550 resuscitated under the right environmental conditions [50]. The highly infectious *L.*
551 *monocytogenes* cause high mortality rate regardless of antibiotic treatments [46]. Listeriosis
552 disease caused by *L. monocytogenes* often leads to rare complications that are highly threatening
553 to human health [51]. As various types of chemical intervention strategies are continuously
554 developed to combat the potent and recurring infectious agents such as *E. coli* and *L.*
555 *monocytogenes*, potential contributions of such intervention strategies to the evolution of
556 resilience among the newly emerged isolates are often overlooked. Acclimation and adaptation
557 to strong selection pressures (supra-optimal effects) triggered by xenobiotic agents must be well
558 understood for more strategic implementation of combinatorial approaches to intervention.
559 With the increasing social and economic burdens caused by bacterial anti-microbial
560 resistance (AMR), the World Health Organization (WHO) reported that significant gaps continue
561 to emerge during the development of a successful anti-microbial stewardship program [52].
562 Given its medical, environmental, and industrial importance, a comprehensive understanding of
563 bacterial response to chemical intervention is essential in combatting bacterial pathogens and
564 their potential global socio-economic impacts. Most studies that investigated how bacterial
565 pathogens respond to chemical hygiene practices mainly focused on developing new strategies to
566 diminish contamination [21]. Our previous studies demonstrated that the efficacy of growth
567 reducing action caused by another chemical intervention agent ClO_2 against *E. coli* on on-host
568 tomato was dependent on dose × time effects [33]. Previous studies have unraveled the cellular
569 and molecular mechanisms of β-lactam antibiotic-induced resistance in *E. coli* [53]. Despite this

570 advance, little is known about the nature of bacterial defense responses triggered by supra-
571 optimal dose × time effects. Effective, and sustainable treatment strategies that reduce
572 contamination of fruits and vegetables have been difficult to achieve, largely due to poor
573 understanding of the molecular genetic mechanisms associated with xenobiotic effects of
574 chemical intervention agents. Fine-tuned strategies that balance the dose x time effects with the
575 need to preserve the sensory and biochemical properties of the fresh produce are critical in
576 preventing the potential supra-optimal effects of xenobiotic agents to bacterial acclimation,
577 adaptation, and even mutation.

578 Our previous studies on the effects of ClO_2 to *E. coli* on non-host tomato environment
579 revealed that supra-optimal exposure time, even at an effective dose, could lead to a second burst
580 of independent defense responses [33]. In particular, the activation of pathogenicity and stress-
581 adaptive genes response with prolonged exposure to a high dose (10 µg) of ClO_2 points to the
582 probable occurrence of adaptation and selection, leading to resistance. However, we observed a
583 new burst of defense responses triggered by a moderate dose of O_3 (2 µg) in *E. coli* at the second
584 hour of exposure (Fig. 2), an indication low dosage of O_3 potentially triggers acclimation and
585 adaptation.

586

587 **Xenobiotic effects of O_3 against *E. coli* and *L. monocytogenes***

588 The potential of gaseous O_3 as a xenobiotic agent for pathogen intervention on foods has
589 been demonstrated [16-18, 54, 55]. In this study, we revealed that O_3 is capable of reducing the
590 level of viable *E. coli* and *L. monocytogenes* inocula on tomato fruits as a non-host vector for
591 transmission to humans [8]. The transcriptional regulatory networks of both *E. coli* and *L.*
592 *monocytogenes* under various conditions have been studied previously [56-60]. We investigated

593 the transcriptional regulatory networks of *E. coli* and *L. monocytogenes* surviving on its non-host
594 tomato after exposure to low (1 µg per gram of fruit), moderate (2 µg per gram of fruit) and high
595 (3 µg per gram of fruit) doses of O_3. Our results indicated that *E. coli* and *L. monocytogenes*
596 respond to O_3 exposure in dosage × time-dependent manner (Fig. 1, 2 and 5). High dose appeared
597 to have the highest potential to trigger adaptation in *E. coli* but not in *L. monocytogenes,*
598 suggesting that *E. coli* has higher basal resistance than *L. monocytogenes* (Fig. 3). In our
599 previous studies, we also reported that another xenobiotic intervention agent ClO_2 induced
600 potential acclimation and adaptation in *E. coli* surviving on fresh tomato [33]. Taking together,
601 our findings suggest that when optimizing xenobiotic intervention procedures, potential bacterial
602 adaptation needs to be taken into consideration while balancing the dose × time effects on the
603 physical and biochemical properties of the fresh produce being subjected to such treatments.
604

605 **The nature of *E. coli* and *L. monocytogenes* response mechanisms to O_3 xenobiosis**

606 We revealed that O_3 caused changes in the expression of genes associated with
607 pathogenicity, stress response, cell motility, transcriptional regulation, primary metabolism, and
608 transport in both *E. coli* and *L. monocytogenes* (Fig. 3). Pathogenicity genes involved in T3SS
609 system (in *E. coli*), T2SS system (in *L. monocytogenes*), biofilm formation, quorum sensing, and
610 two-component system were triggered during exposure to O_3 (Fig. 5; Additional file 2: Table
611 S1). When *E. coli* was exposed to a high dose of O_3, upregulation of genes associated with those
612 functions occurred largely during the short-term (1 hr) exposure, but such pattern of gene activity
613 was not observed during prolonged exposure. In our previous study, we also observed changes in
614 expression of T3SS system, biofilm formation, quorum sensing, and two-component system
615 genes during exposure to ClO_2 in *E. coli* [33].

T3SS genes involved in virulence (ECs4590, ECs3730, ECs3731, ECs3732, ECs3733, ECs3726, ECs3725, ECs3724 and ECs3721) were upregulated during short-term (1 hr) exposure to a high dose but downregulated with prolonged exposure up to 2 hr. Suppression of defense response was likely due to a significant reduction in metabolic activity, concurrent with partial or complete arrest of cell division [61] (Fig. 1A). The substantial similarities in the transcriptional changes in *E. coli* during moderate (2 hr) and longer (3 hr) exposure times but not with shorter (1 hr) exposure time indicated that longer exposure could potentially cause a selection pressure that could trigger acclimation and adaptation. The apparent exposure time-dependence of gene expression in *E. coli* under a high dose suggested that toxicity effects, as well as genetic mechanisms, might be different at various periods during xenobiosis. In contrast, these changes were not observed in *L. monocytogenes*, indicating adaptation is not likely induced in the Gram-positive bacteria as implied by the nature of its transcriptional networks (Fig. 3 and 6).

Acclimation of *E. coli* and *L. monocytogenes* due to chronic effects

Our previous study showed significant changes in transcriptional regulatory networks in *E. coli* in response to ClO_2 treatment as indicators of either defenses or acclimation [33]. In this study, systematic reconstruction of the transcriptional regulatory networks across different dosages of O_3 (*i.e.*, 1 μg, 2 μg, 3 μg) showed that gene modules associated with pathogenicity, stress response, transcriptional regulation, and transport processes play important roles in defense against O_3 xenobiosis (Additional file 3: Table S2). In *E. coli*, prophage induction is often coupled with enhanced virulence and increased tolerance to harsh environmental stresses [62, 63]. The *E. coli* transcriptome data revealed a total of 196 prophage-associated genes to be differentially expressed across different doses and exposure times (Additional file 2: Table S1),

639 indicating that prophage induction plays a critical role in the responses of *E. coli* to O_3-mediated
640 xenobiosis.

641 Current thinking supports that exposure to environmental stresses could stimulate
642 mechanisms that enhance bacterial survival across different host or non-host environments, *i.e.,*
643 stress priming effects [23, 24]. In *E. coli*, it is known that stress could induce acclimation,
644 adaptation, selection, or even rare mutation events. Environmentally induced changes in fitness
645 could lead to selection and population shift that build a novel inoculum with newly acquired
646 tolerance to different modes of intervention. One example is that *E. coli* O157 is more resistant
647 to acid once it is primed by heat treatment [25]. Cross-protection against other stresses induced
648 by salt for example, has also been reported in *L. monocytogenes* in a temperature-dependent
649 manner [64]. Whether O_3 causes mutagenic effects and subsequently contributes to cross-
650 protection mechanisms in *E. coli* or *L. monocytogenes* is unknown. From a food safety
651 standpoint, introducing combinations of relatively mild chemical treatments (*i.e.,* optimal
652 cocktail) might be an attractive alternative to effectively control bacterial pathogens without
653 promoting adaptation or mutation, which are the main causes of perennial outbreaks.

654 Studies have shown that various types of stresses induce changes in gene expression in *E.*
655 *coli* in both pure culture and non-host environments, such as fresh lettuce [48, 65]. In this study,
656 we examined the dynamics of transcriptional co-expression networks of *E. coli* and *L.*
657 *monocytogenes* in line with their responses to different doses of O_3 on non-host tomato surface,
658 which may serve as a pre-exposure to another stressor causing either cross-protection or cross-
659 vulnerability [24]. We found that the genetic network configurations of *E. coli* and *L.*
660 *monocytogenes* are very flexible under different doses of O_3 over short or longer duration of
661 exposure. We also characterized the transcriptional changes in *E. coli* and *L. monocytogenes*

662 growing in pure culture and on tomato surface, providing great reference transcriptomes on these
663 pathogens growing on various substrates (Additional file 2: Table S1).

664 We previously reported that the transcriptional regulatory network of *E. coli* in response
665 to a low dose of ClO_2 is controlled by a *putative endopeptidase* (ECs2739) as a central hub,
666 likely through its functions associated with stress signaling, antibiotic binding and recognition,
667 bacteriophage activity, and morphology determination [66, 67]. In this study, no putative central
668 hub or core regulator was apparent for the O_3 response networks of both *E. coli* and *L.*
669 *monocytogenes*. However, it is apparent that the responses and associated mechanisms triggered
670 by O_3 xenobiosis are distinct from the responses triggered by ClO_2. The *putative endopeptidase*
671 gene that serves as the central hub in the ClO_2 networks of *E. coli* was downregulated by 1 µg O_3
672 at 3 hr and 3 µg O_3 at 2 hr, but upregulated under 1 µg and 2 µg O_3 at 2 hr, and 3 µg O_3 at 3 hr
673 (Additional file 2: Table S1). Such response mimics the typical profile of biological invasion that
674 often involves the degradation of foreign proteins by enhanced endopeptidase activities [68, 69].

675 The current study illustrates the power of transcriptome profiling for understanding the
676 genetic networks involved in the responses of pathogenic bacteria (*E. coli*, *L. monocytogenes*) to
677 sub-optimal, optimal, or supra-optimal effects of a potential xenobiotic agent (O_3) used for
678 intervention in food processing. We have established a platform to investigate the molecular
679 mechanisms underlying pathogen interaction with intervention chemicals, providing a baseline
680 for optimizing dose × time dynamics for maximal efficacy [33]. The differentially expressed
681 genes could serve as targets in both *E. coli* and *L. monocytogenes* for future development of
682 novel strategies for controlling foodborne pathogens, including the use of new chemical and bio-
683 control agents, *i.e.*, non-toxic and non-pathogenic biocontrol bacterial strains or phage can be
684 considered. In addition, means for tricking the signal transduction pathways associated with

685 defense response to various chemicals could be an alternative strategy to re-wire the bacterial
686 genetic networks, thereby reducing selective pressure and avoiding the emergence of chemical-
687 tolerant inocula. The information generated in this study also provides an important resource for
688 further research in food safety and foodborne pathogen epidemiology.
689
690 **Conclusions**
691 The present study provides a proof-of-concept on the potential xenobiotic effects of O_3 to
692 *E. coli* but not in *L. monocytogenes* and the importance of dose × time dynamics for optimal
693 intervention. The paradigm of this study could be applied to evaluate the impacts of different
694 intervention strategies in the food industry to eliminate bacterial pathogens surviving in fresh
695 produce while minimizing the negative consequences on selection and adaptation.
696
697 **Data deposition**
698 RNA-Seq data were deposited in the National Center for Biotechnology Information
699 (NCBI) Sequence Read Archive (SRA) collection under the accession number SRR8468286-9.
700
701 **List of abbreviations**
702 AMR: antimicrobial resistance; ClO_2: chlorine dioxide; CT-SMAC: MacConkey Sorbital Agar
703 supplemented with Cefixime and Tellurite; *E. coli*: *Escherichia coli*; hr: hour(s); *HSP*: *heat*
704 *shock protein*; *L. monocytogenes*: Listeria *monocytogenes*; NaB: sodium benzoate; NaClO:
705 sodium hypochlorite; $NaClO_2$: sodium chlorite; NCBI: National Center for Biotechnology
706 Information; O_3: ozone; PAA: peracetic acid; PCC: Pearson Correlation Coefficient; PS:
707 propensity score; RNA-Seq: RNA-Sequencing; RPKM: Reads Per Kilobase of transcript, per

Million mapped reads; SRA: Sequence Read Archive; STEC: Shiga toxin-producing *Escherichia coli*; T2SS: type II secretion system; T3SS: type III secretion system; TSA: tryptic soy agar; USDA: the U.S. Department of Agriculture; VBNC: viable but non-culturable; WHO: World Health Organization.

Ethics approval and consent to participate

Not applicable

Consent for publication

Not applicable

Availability of data and materials

Sequence files are available at NCBI SRA under accession number SRR8468286-9.

Competing interests

The authors declare that they have no competing interests.

Funding

This work was supported by the United States Department of Agriculture, National Institute of Food and Agriculture, Agriculture and Food Research Initiative (USDA-NIFA-AFRI) Grant 2015-69003-32075, USDA-ARS CRIS projects 2030-42000-055-00D, and Bayer Crop Science Endowed Professorship Funds to BGDR.

Authors' contributions

BGDR and VW conceptualized and supervised the whole study. BGDR and XS interpreted the data and co-wrote the manuscript. MS, DB and VW performed all the microbial works and chemical treatments and prepared all the samples for RNA-Seq libraries. AK designed the RNA-Seq experiments and assembled the Illumina sequence reads. XS, MS and NBRK performed the biological interrogation and analysis of the RNA-Seq data. XS and NBRK performed all bio-computing works, statistical analyses, and genetic network modeling.

Acknowledgments

We thank the ROIS supercomputing facilities of the National Institute of Genetics (Mishima, Japan) for the access to their RNA-Seq assembly pipeline for the assembly of the bacterial transcriptomic data generated in this study.

References

1. Nataro JP, Kaper JB. Diarrheagenic Escherichia coli. Clin Microbiol Rev. 1998;11(0893-8512 (Print)):142-201.
2. Santiago AE, Yan MB, Hazen TH, Sauder B, Meza-Segura M, Rasko DA, et al. The AraC Negative Regulator family modulates the activity of histone-like proteins in pathogenic bacteria. PLoS Pathog 2017;13(1553-7374 (Electronic)):e100654. doi: 10.1371/journal.ppat.1006545.
3. Law D. Virulence factors of Escherichia coli O157 and other Shiga toxin-producing E. coli. Journal of Applied Microbiology. 2001;88(5):729-45. doi: 10.1046/j.1365-2672.2000.01031.x.
4. Rivera-Betancourt M, D. SS, M. AT, E. WK, G. B, M. R, et al. Prevalence of Escherichia coli O157:H7, Listeria monocytogenes, and Salmonella in two geographically distant commercial beef processing plants in the United States. J Food Prot. 2004;67(0362-028X (Print)):295-302. doi: 10.4315/0362-028x-67.2.295.
5. Mead PS, L. S, V. D, F. ML, S. BJ, C. S, et al. Food-related illness and death in the United States. Emerg Infect Dis. 1999;5(1080-6040 (Print)):607-25. doi: 10.3201/eid0505.990502.
6. Watanabe H, Wada A, Inagaki Y, Itoh K-I, Tamura K. Outbreaks of enterohaemorrhagic Escherichia coli O157:H7 infection by two different genotype strains in Japan, 1996. The Lancet. 1996;348(9030):831-2. doi: 10.1016/S0140-6736(05)65257-9.
7. Gomez-Aldapa CA, Torres-Vitela Mdel R, Acevedo-Sandoval OA, Rangel-Vargas E, Villarruel-Lopez A, Castro-Rosas A. Presence of Shiga toxin-producing Escherichia coli, Enteroinvasive E. coli,

763 Enteropathogenic E. coli, and Enterotoxigenic E. coli on tomatoes from public markets in Mexico. J Food
764 Prot. 2013;76(1944-9097 (Electronic)):1621-5. doi: 10.4315/0362-028X.JFP-13-071.
765 8. Bridges DF, Rane B, Wu VCH. The effectiveness of closed-circulation gaseous chlorine dioxide or
766 ozone treatment against bacterial pathogens on produce. Food Control. 2018;91:261-7. doi:
767 10.1016/j.foodcont.2018.04.004.
768 9. Hwang C-A, Huang L, Wu WC-H. In Situ Generation of Chlorine Dioxide for Surface
769 Decontamination of Produce. Journal of Food Protection. 2017;80(4):567-72. doi: 10.4315/0362-
770 028x.Jfp-16-367. PubMed PMID: 28272919.
771 10. Cai S, Worobo RW, Snyder AB. Outgraded produce variably retains surface inoculated
772 Escherichia coli through washing. Int J Food Microbiol. 2018;269(1879-3460 (Electronic)):27-35. doi:
773 10.1016/j.ijfoodmicro.2018.01.012.
774 11. Yeni F, Yavas S, Alpas H, Soyer Y. Most Common Foodborne Pathogens and Mycotoxins on Fresh
775 Produce: A Review of Recent Outbreaks. Crit Rev Food Sci Nutr 2016;56(1549-7852 (Electronic)):1532-
776 44. doi: 10.1080/10408398.2013.777021.
777 12. Cadieux B, Colavecchio A, Jeukens J, Freschi, Emond-Rheault J-G, Kukavica-Ibrulj I, et al.
778 Prophage induction reduces Shiga toxin producing Escherichia coli (STEC) and Salmonella enterica on
779 tomatoes and spinach: A model study. Food Control. 2018;89:250-9. doi:
780 10.1016/j.foodcont.2018.02.001.
781 13. Chen H, Zhong Q. Antibacterial activity of acidified sodium benzoate against Escherichia coli
782 O157:H7, Salmonella enterica, and Listeria monocytogenes in tryptic soy broth and on cherry tomatoes.
783 Int J Food Microbiol. 2018;274(1879-3460 (Electronic)):38-44. doi: 10.1016/j.ijfoodmicro.2018.03.017.
784 14. Singh P, Hung YC, Qi H. Efficacy of Peracetic Acid in Inactivating Foodborne Pathogens on Fresh
785 Produce Surface. J Food Sci 2018;83(1750-3841 (Electronic)):432-9. doi: 10.1111/1750-3841.14028.
786 15. Fan X, Sokorai KJB, Engemann J, Gurtler JB, Liu Y. Inactivation of Listeria innocua, Salmonella
787 Typhimurium, and Escherichia coli O157:H7 on Surface and Stem Scar Areas of Tomatoes Using In-
788 Package Ozonation. Journal of Food Protection. 2012;75(9):1611-8. doi: 10.4315/0362-028X.JFP-12-103.
789 16. Trinetta V, Vaidya N, Linton R, Morgan M. A comparative study on the effectiveness of chlorine
790 dioxide gas, ozone gas and e-beam irradiation treatments for inactivation of pathogens inoculated onto
791 tomato, cantaloupe and lettuce seeds. International Journal of Food Microbiology. 2011;146(2):203-6.
792 doi: 10.1016/j.ijfoodmicro.2011.02.014.
793 17. de Oliveira Souza SM, de Alencar ER, Ribeiro JL, de Aguiar Ferreira M. Inactivation of Escherichia
794 coli O157:H7 by ozone in different substrates. Brazilian Journal of Microbiology. 2019;50(1):247-53. doi:
795 10.1007/s42770-018-0025-2.
796 18. Liu T, Wang D, Liu H, Zhao W, Wang W, Shao L. Rotating packed bed as a novel disinfection
797 contactor for the inactivation of E. coli by ozone. Chemosphere. 2019;214:695-701. doi:
798 10.1016/j.chemosphere.2018.09.149.
799 19. Asakura H, Igimi S, Kawamoto K, Yamamoto S, Makino S. Role of in vivo passage on the
800 environmental adaptation of enterohemorrhagic Escherichia coli O157:H7: cross-induction of the viable
801 but nonculturable state by osmotic and oxidative stresses. FEMS Microbiol Lett. 2005;253(0378-1097
802 (Print)):243-9.
803 20. Phan-Thanh L, Mahouin F, Aligé S. Acid responses of Listeria monocytogenes. International
804 Journal of Food Microbiology. 2000;55(1):121-6. doi: https://doi.org/10.1016/S0168-1605(00)00167-7.
805 21. Pu Y, Zhao Z, Li Y, Zou J, Ma Q, Zhao Y, et al. Enhanced efflux activity facilitates drug tolerance in
806 dormant bacterial cells. Molecular cell. 2016;62(2):284-94. doi: 10.1016/j.molcel.2016.03.035. PubMed
807 PMID: 27105118.
808 22. Fletcher S. Understanding the contribution of environmental factors in the spread of
809 antimicrobial resistance. Environ Health Prev Med. 2015;20(4):243-52. Epub 2015/04/29. doi:
810 10.1007/s12199-015-0468-0. PubMed PMID: 25921603.

811 23. Gunasekera TS, Csonka LN, Paliy O. Genome-Wide Transcriptional Responses of Escherichia coli
812 K-12 to Continuous Osmotic and Heat Stresses. Journal of Bacteriology. 2008;190(10):3712-20. doi:
813 10.1128/JB.01990-07. PubMed PMID: PMC2395010.
814 24. Zorraquino V, Kim M, Rai N, Tagkopoulos I. The Genetic and Transcriptional Basis of Short and
815 Long Term Adaptation across Multiple Stresses in Escherichia coli. Molecular Biology and Evolution.
816 2017;34(3):707-17. doi: 10.1093/molbev/msw269.
817 25. Wang G, Doyle MP. Survival of enterohemorrhagic Escherichia coli O157:H7 in water. J Food
818 Prot. 1998;61(0362-028X (Print)):662-7.
819 26. Shu X, Singh M, Karampudi NBR, Bridges DF, Kitazumi A, Wu VCH, et al. Xenobiotic Effects of
820 Chlorine Dioxide to Escherichia coli O157:H7 on Non-host Tomato Environment Revealed by
821 Transcriptional Network Modeling: Implications to Adaptation and Selection. Frontiers in Microbiology.
822 2020;11:1122.
823 27. Li J, Liu L, Yang D, Liu WL, Shen ZQ, Qu HM, et al. Culture-dependent enumeration methods
824 failed to simultaneously detect disinfectant-injured and genetically modified Escherichia coli in drinking
825 water. Environ Sci Process Impacts. 2017;19(2050-7895 (Electronic)):720-6. doi: 10.1039/c6em00625f.
826 28. Shu X, Livingston DP, Woloshuk CP, Payne GA. Comparative Histological and Transcriptional
827 Analysis of Maize Kernels Infected with Aspergillus flavus and Fusarium verticillioides. Frontiers in Plant
828 Science. 2017;8:2075. doi: 10.3389/fpls.2017.02075.
829 29. Kitazumi A, Pabuayon ICM, Ohyanagi H, Fujita M, Osti B, Shenton MR, et al. Potential of *Oryza*
830 *officinalis* to augment the cold tolerance genetic mechanisms of *Oryza sativa* by network
831 complementation. Nature Scientific Reports. 2018;8:16346. doi: 10.1038/s41598-018-34608-z.
832 30. Martin M. Cutadapt removes adapter sequences from high-throughput sequencing reads.
833 EMBnetjournal. 2011;17:10. doi: 10.14806/ej.17.1.200.
834 31. Magoc T, Wood D, Salzberg SL. EDGE-pro: Estimated Degree of Gene Expression in Prokaryotic
835 Genomes. Evolutionary bioinformatics online. 2013;9:127-36. doi: 10.4137/EBO.S11250. PubMed PMID:
836 23531787.
837 32. Kanehisa M, Goto S. Metabolomic and transcriptomic stress response of Escherichia coli. Nucleic
838 Acids Research. 2000;28(1):27-30. doi: 10.1038/msb.2010.18. PubMed PMID: PMC102409.
839 33. Shu X, Singh M, Bhushana NB, Bridges DF, Kitazumi A, Wu VCH, et al. Elucidating effects of
840 chlorine dioxide on global transcriptional networks in *Escherichia coli* O157:H7 on non-host tomato.
841 Front Microbiol. 2020;11:1122. doi: 10.3389/fmicb.2020.01122.
842 34. McAteer SP, Sy BM, Wong JL, Tollervey D, Gally DL, Tree JJ. Ribosome maturation by the
843 endoribonuclease YbeY stabilizes a type 3 secretion system transcript required for virulence of
844 enterohemorrhagic Escherichia coli. J Biol Chem 2018;293(1083-351X (Electronic)):9006-16. doi:
845 10.1074/jbc.RA117.000300.
846 35. Ng W-L, Bassler BL. Bacterial Quorum-Sensing Network Architectures. Annual Review of
847 Genetics. 2009;43(1):197-222. doi: 10.1146/annurev-genet-102108-134304.
848 36. Breland EJ, Eberly AR, Hadjifrangiskou M. An Overview of Two-Component Signal Transduction
849 Systems Implicated in Extra-Intestinal Pathogenic E. coli Infections. Frontiers in Cellular and Infection
850 Microbiology. 2017;7:162. doi: 10.3389/fcimb.2017.00162. PubMed PMID: PMC5422438.
851 37. Rodionova IA, Zhang Z, Mehla J, Goodacre N, Babu M, Emili A, et al. The phosphocarrier protein
852 HPr of the bacterial phosphotransferase system globally regulates energy metabolism by directly
853 interacting with multiple enzymes in Escherichia coli. The Journal of biological chemistry.
854 2017;292(34):14250-7. Epub 2017/06/20. doi: 10.1074/jbc.M117.795294. PubMed PMID: 28634232.
855 38. Wang S, Yang F, Yang B. Global effect of CsrA on gene expression in enterohemorrhagic
856 Escherichia coli O157:H7. Research in Microbiology. 2017;168(8):700-9. doi:
857 10.1016/j.resmic.2017.08.003.

858 39. Yang B, Jiang L, Wang S, Wang L. Global transcriptional regulation by BirA in enterohemorrhagic
859 Escherichia coli O157:H7. Future Microbiol. 2018;13:757-69. doi: 10.2217/fmb-2017-0256.
860 40. Redford P, Welch RA. Role of Sigma E-Regulated Genes in Escherichia coli Uropathogenesis.
861 Infection and Immunity. 2006;74(7):4030-8. doi: 10.1128/IAI.01984-05. PubMed PMID: PMC1489677.
862 41. Wilson JW, Schurr MJ, LeBlanc CL, Ramamurthy R, Buchanan KL, Nickerson CA. Mechanisms of
863 bacterial pathogenicity. Postgraduate Medical Journal. 2002;78(918):216. doi: 10.1136/pmj.78.918.216.
864 42. Otto M. *Staphylococcus aureus* toxins. Current opinion in microbiology. 2014;17:32-7. Epub
865 2013/12/10. doi: 10.1016/j.mib.2013.11.004. PubMed PMID: 24581690.
866 43. Churchill RLT, Lee H, Hall JC. Detection of *Listeria monocytogenes* and the toxin listeriolysin O in
867 food. Journal of microbiological methods. 2006;64(2):141-70. Epub 2005/11/28. doi:
868 10.1016/j.mimet.2005.10.007. PubMed PMID: 16310269.
869 44. Martinović T, Andjelković U, Gajdošik MŠ, Rešetar D, Josić D. Foodborne pathogens and their
870 toxins. Journal of proteomics. 2016;147:226-35. Epub 2016/04/22. doi: 10.1016/j.jprot.2016.04.029.
871 PubMed PMID: 27109345.
872 45. Robin LTC, Lee H, Hall JC. Detection of Listeria monocytogenes and the toxin listeriolysin O in
873 food. Journal of Microbiological Methods. 2006;64(2):141-70. doi:
874 https://doi.org/10.1016/j.mimet.2005.10.007.
875 46. Thønnings S, Knudsen JD, Schønheyder HC, Søgaard M, Arpi M, Gradel KO, et al. Antibiotic
876 treatment and mortality in patients with Listeria monocytogenes meningitis or bacteraemia. Clinical
877 Microbiology and Infection. 2016;22(8):725-30. doi: https://doi.org/10.1016/j.cmi.2016.06.006.
878 47. Tuttle J, Gomez T, Doyle MP, Wells JG, Zhao T, Tauxe RV, et al. Lessons from a large outbreak of
879 Escherichia coli O157:H7 infections: insights into the infectious dose and method of widespread
880 contamination of hamburger patties. Epidemiol Infect. 1999;122(0950-2688 (Print)):185-92.
881 48. Allen KJ, Griffiths MW. Impact of hydroxyl- and superoxide anion-based oxidative stress on
882 logarithmic and stationary phase Escherichia coli O157:H7 stress and virulence gene expression. Food
883 Microbiol. 2012;29(1095-9998 (Electronic)):141-7. doi: 10.1016/j.fm.2011.09.014.
884 49. Chekabab SM, Jubelin G, Dozois CM, Harel J. PhoB Activates Escherichia coli O157:H7 Virulence
885 Factors in Response to Inorganic Phosphate Limitation. PLoS ONE. 2014;9(4):e94285. doi:
886 10.1371/journal.pone.0094285. PubMed PMID: PMC3978041.
887 50. Gullian-Klanian M, Sanchez-Solis MJ. Growth kinetics of Escherichia coli O157:H7 on the epicarp
888 of fresh vegetables and fruits. Braz J Microbiol 2018;49(1678-4405 (Electronic)):104-11. doi:
889 10.1016/j.bjm.2017.08.001.
890 51. Canham LJW, Manara A, Fawcett J, Rolinski M, Mortimer A, Inglis KEA, et al. Mortality from
891 Listeria monocytogenes meningoencephalitis following escalation to alemtuzumab therapy for
892 relapsing-remitting Multiple Sclerosis. Multiple Sclerosis and Related Disorders. 2018;24:38-41. doi:
893 https://doi.org/10.1016/j.msard.2018.05.014.
894 52. Organization WH. Antimicrobial resistance global report on surveillance. Geneva.
895 2014;Switzerland.
896 53. Akhavan BJ, Vijhani P. Amoxicillin: Treasure Island (FL): StatPearls Publishing; 2020.
897 54. Iakovides IC, Michael-Kordatou I, Moreira NFF, Ribeiro AR, Fernandes T, Pereira MFR, et al.
898 Continuous ozonation of urban wastewater: Removal of antibiotics, antibiotic-resistant Escherichia coli
899 and antibiotic resistance genes and phytotoxicity. Water Research. 2019;159:333-47. doi:
900 10.1016/j.watres.2019.05.025.
901 55. Hu Y, Oliver HF, Raengpradub S, Palmer ME, Orsi RH, Wiedmann M, et al. Transcriptomic and
902 phenotypic analyses suggest a network between the transcriptional regulators HrcA and sigmaB in
903 Listeria monocytogenes. Appl Environ Microbiol. 2007;73(1098-5336 (Electronic)):7981-91.

904 56. Wang J, Chen L, Tian X, Gao L, Niu X, Shi M, et al. Global Metabolomic and Network analysis of
905 Escherichia coli Responses to Exogenous Biofuels. Journal of Proteome Research. 2013;12(11):5302-12.
906 doi: 10.1021/pr400640u.
907 57. Santos-Zavaleta A, Sánchez-Pérez M, Salgado H, Velázquez-Ramírez DA, Gama-Castro S,
908 Tierrafría VH, et al. A unified resource for transcriptional regulation in Escherichia coli K-12 incorporating
909 high-throughput-generated binding data into RegulonDB version 10.0. BMC Biology. 2018;16:91. doi:
910 10.1186/s12915-018-0555-y. PubMed PMID: PMC6094552.
911 58. Perna NT, Plunkett Iii G, Burland V, Mau B, Glasner JD, Rose DJ, et al. Genome sequence of
912 enterohaemorrhagic Escherichia coli O157:H7. Nature. 2001;409:529-33. doi: 10.1038/35054089.
913 59. Bando SY, Iamashita P, Guth BE, Dos Santos LF, Fujita A, Abe CM, et al. A hemolytic-uremic
914 syndrome-associated strain O113:H21 Shiga toxin-producing Escherichia coli specifically expresses a
915 transcriptional module containing dicA and is related to gene network dysregulation in Caco-2 cells.
916 PLoS One 2017;12(1932-6203 (Electronic)):e0189613. doi: 10.1371/journal.pone.0189613.
917 60. Hurley D, Luque-Sastre L, Parker CT, Huynh S, Eshwar AK, Nguyen SV, et al. Whole-Genome
918 Sequencing-Based Characterization of 100 Listeria monocytogenes Isolates Collected from Food
919 Processing Environments over a Four-Year Period. LID - 10.1128/mSphere.00252-19 [doi] LID - e00252-
920 19. mSphere. 2019;4(2379-5042 (Electronic)):e00252-19. doi: 10.1128/mSphere.00252-19.
921 61. Jozefczuk S, Klie S, Catchpole G, Szymanski J, Cuadros-Inostroza A, Steinhauser D, et al.
922 Metabolomic and transcriptomic stress response of Escherichia coli. Molecular Systems Biology.
923 2010;6:364-. doi: 10.1038/msb.2010.18. PubMed PMID: PMC2890322.
924 62. Li D, Tang F, Xue F, Ren J, Liu Y, Yang D, et al. Prophage phiv142-3 enhances the colonization and
925 resistance to environmental stresses of avian pathogenic Escherichia coli. Veterinary Microbiology.
926 2018;218:70-7. doi: 10.1016/j.vetmic.2018.03.017.
927 63. Fang Y, Mercer RG, McMullen LM, Gänzle MG. Induction of Shiga Toxin-Encoding Prophage by
928 Abiotic Environmental Stress in Food. Appl Environ Microbiol. 2017;83(19):e01378-17. doi:
929 10.1128/AEM.01378-17. PubMed PMID: 28778890.
930 64. Bergholz TM, Bowen B, Wiedmann M, Boor KJ. Listeria monocytogenes shows temperature-
931 dependent and -independent responses to salt stress, including responses that induce cross-protection
932 against other stresses. Appl Environ Microbiol. 2012;78(8):2602-12. Epub 2012/02/03. doi:
933 10.1128/AEM.07658-11. PubMed PMID: 22307309.
934 65. Mei G-Y, Tang J, Bach S, Kostrzynska M. Changes in Gene Transcription Induced by Hydrogen
935 Peroxide Treatment of Verotoxin-Producing Escherichia coli O157:H7 and Non-O157 Serotypes on
936 Romaine Lettuce. Frontiers in Microbiology. 2017;8:477. doi: 10.3389/fmicb.2017.00477.
937 66. Meberg BM, Paulson AL, Priyadarshini R, Young KD. Endopeptidase penicillin-binding proteins 4
938 and 7 play auxiliary roles in determining uniform morphology of Escherichia coli. Journal of bacteriology.
939 2004;186(24):8326-36. doi: 10.1128/JB.186.24.8326-8336.2004. PubMed PMID: 15576782.
940 67. Lood R, Molina H, Fischetti VA. Determining bacteriophage endopeptidase activity using either
941 fluorophore-quencher labeled peptides combined with liquid chromatography-mass spectrometry (LC-
942 MS) or Förster resonance energy transfer (FRET) assays. PloS one. 2017;12(3):e0173919-e. doi:
943 10.1371/journal.pone.0173919. PubMed PMID: 28296948.
944 68. Chang GR-L, Wang M-Y, Liao J-H, Hsiao Y-P, Lai S-Y. Endopeptidase activity characterization of E.
945 coli-derived infectious bursal disease virus protein 4 tubules. Protein Engineering, Design and Selection.
946 2012;25(11):789-95. doi: 10.1093/protein/gzs087.
947 69. Kashyap DR, Kuzma M, Kowalczyk DA, Gupta D, Dziarski R. Bactericidal peptidoglycan
948 recognition protein induces oxidative stress in Escherichia coli through a block in respiratory chain and
949 increase in central carbon catabolism. Molecular microbiology. 2017;105(5):755-76. doi:
950 10.1111/mmi.13733. PubMed PMID: PMC5570643.

951

952

953

954

955

956

957

958

959

960

961

962

963

964

965

966

967

968

969

970

971

972

973 **List of Figures**

974 **Figure 1.** Growth reduction of *E. coli* **(A)** and *L. monocytogenes* **(B)** on non-host tomato treated
975 with different doses of gaseous ozone (O_3). Tomatoes harboring bacterial cells were treated with
976 1 µg, 2 µg, and 3 µg O_3 per gram of ripe fruits. Capital letters indicate significant difference ($P <$
977 0.05) caused by O_3 doses at the same time-point. Lowercase letters indicate significant difference
978 ($P < 0.05$) caused by time of exposure under the same O_3 dosage. (PowerPoint 106 KB)

979

980 **Figure 2.** Dynamic changes in the *E. coli* O157:H7 and *L. monocytogenes* transcriptomes as an
981 effect of different doses of O_3 treatments. **(A and B)** Scatter plots of the Propensity Scores (PS)
982 for each transcriptome library in *E. coli* O157:H7 **(A)** and *L. monocytogenes* **(B)**. **(C and D)**
983 Total numbers of *E. coli* **(C)** and *L. monocytogenes* **(D)** genes that were differentially expressed
984 in response to 1 µg, 2 µg, and 3 µg of O_3 per gram of ripe tomato after 1 hr, 2 hr, and 3 hr
985 exposure at each dose. Total numbers of upregulated (↑) and downregulated (↓) genes that were
986 either treatment-specific or shared between treatments are displayed in the Venn diagrams.
987 (PowerPoint 733 KB)

988

989 **Figure 3.** Functional categories of genes in *E. coli* O157:H7 **(A)** and *L. monocytogenes* **(B)** that
990 were differentially expressed at a different duration of exposure (1 hr, 2 hr, 3 hr) to O_3. Colored
991 bars represent the numbers of differentially expressed genes assigned to each functional
992 category. Positive bars denote the number of upregulated genes. Negative bars denote the
993 number of downregulated genes. Genes assigned to 'other category' and 'unknown' are not
994 included in this figure. (PowerPoint 111 KB)

995

996 **Figure 4.** Two-way hierarchical clustering of differentially expressed *E. coli* **(A)** and *L.*
997 *monocytogenes* **(B)** genes. Ward's Hierarchical Clustering was performed to analyze the
998 Propensity Scores (PS) (left) and RPKM values (right) of bacterial genes in response to O_3
999 treatments after 1 hr, 2 hr and 3 hr exposure. The number of clusters was set at 20 with color-
1000 coding, as shown in detail Additional file 2: Table S1. Red indicates high expression and green
1001 indicates low expression. (PowerPoint 163 KB)

1002

1003 **Figure 5.** Heat map of differentially expressed *E. coli* **(A)** and *L. monocytogenes* **(B)** genes
1004 associated with pathogenesis and stress response. PS of genes in response to O_3 treatments after
1005 1 hr, 2 hr and 3 hr were plotted. Red indicates high expression and green indicates low
1006 expression. (PowerPoint 122 KB)

1007

1008 **Figure 6.** Models of transcriptional co-expression networks constructed for *E. coli* **(A)** and *L.*
1009 *monocytogenes* **(B),** based on co-expression under control (untreated), and 1 hr, 2 hr, and 3 hr
1010 exposure to different doses of O_3. Each node represents a gene and each line denotes the
1011 expression correlation between the two nodes. Green node denotes upregulated genes; blue node
1012 denotes downregulated genes; brown line denotes positively correlated genes by Pearson
1013 Correlation Coefficient (PCC); green line denotes negatively correlated genes by PCC.
1014 (PowerPoint 2,172 KB)

1015

1016

1017

Additional files

Additional file 1: Figure S1 Scatter plots of the RPKM values for each transcriptome library of *E. coli* **(A)** and *L. monocytogenes* **(B)** in response to 1, 2 and 3 µg of O_3 per gram of ripen fruits at 1 hour (hr), 2 hr and 3 hr, respectively, including the control and pure culture. (PowerPoint 521 KB)

Additional file 2: Table S1 Sheet 1 Significance (up or down-regulated based on Pearson Correlation Coefficient), propensity and RPKM of *E. coli* genes during treatment of 1, 2, and 3 µg of O3 after 1, 2, and 3 hour (hr). **Sheet 2** Significance (up or down-regulated based on Pearson Correlation Coefficient), propensity and RPKM of *L. monocytogenes* genes during treatment of 1, 2, and 3 µg of O3 after 1, 2, and 3 hour (hr). The clusters in columns AN and AQ were shown in Fig. 4. (XLSX 1,139 KB)

Additional file 3: Table S2 Sheet 1 Propensity of *E. coli* genes selected for 1 µg O_3 network analysis. The 250 most highly expressed and 250 most lowly expressed genes from each treatment [control, 1, 2, and 3 hour (hr)]. Label numbers from 0 to 19 denote genes from most lowly expressed to most highly expressed. Only those fall into either label 0 or 19 at least in one treatment were selected. Genes differentially expressed based on Pearson Correlation Coefficient (PCC) were shown in columns L-N. **Sheet 2** Propensity of *E. coli* genes selected for 2 µg O_3 network analysis. The 250 most highly expressed and 250 most lowly expressed genes from each treatment [control, 1, 2 and 3 hour (hr)]. Label numbers from 0 to 19 denote genes from most lowly expressed to most highly expressed. Only those fall into either label 0 or 19 at least in one treatment were selected. Genes differentially expressed based on PCC were shown in columns L-

N. **Sheet 3** Propensity of *E. coli* genes selected for 3 μg O_3 network analysis. The 250 most highly expressed and 250 most lowly expressed genes from each treatment [control, 1, 2 and 3 hour (hr)]. Label numbers from 0 to 19 denote genes from most lowly expressed to most highly expressed. Only those fall into either label 0 or 19 at least in one treatment were selected. Genes differentially expressed based on Pearson Correlation Coefficient were shown in columns L-N. **Sheet 4** Co-expression network of *E. coli* genes for 1 μg O_3 at 1 hr. 'color': 'brown' demotes positively correlated by PCC; 'color': 'green' demotes negatively correlated by PCC. **Sheet 5** Co-expression network of *E. coli* genes for 1 μg O_3 at 2 hr. 'color': 'brown' demotes positively correlated by PCC; 'color': 'green' demotes negatively correlated by PCC. **Sheet 6** Co-expression network of *E. coli* genes for 1 μg O_3 at 3 hr. 'color': 'brown' demotes positively correlated by PCC; 'color': 'green' demotes negatively correlated by PCC. **Sheet 7** Co-expression network of *E. coli* genes for 1 μg O_3 control. 'color': 'brown' demotes positively correlated by PCC; 'color': 'green' demotes negatively correlated by PCC. **Sheet 8** Co-expression network of *E. coli* genes for 2 μg O_3 at 1 hr. 'color': 'brown' demotes positively correlated by PCC; 'color': 'green' demotes negatively correlated by PCC. **Sheet 9** Co-expression network of *E. coli* genes for 2 μg O_3 at 2 hr. 'color': 'brown' demotes positively correlated by PCC; 'color': 'green' demotes negatively correlated by PCC. **Sheet 10** Co-expression network of *E. coli* genes for 2 μg O_3 at 3 hr. 'color': 'brown' demotes positively correlated by PCC; 'color': 'green' demotes negatively correlated by PCC. **Sheet 11** Co-expression network of *E. coli* genes for 2 μg O_3 control. 'color': 'brown' demotes positively correlated by PCC; 'color': 'green' demotes negatively correlated by PCC. **Sheet 12** Co-expression network of *E. coli* genes for 3 μg O_3 at 1 hr. 'color': 'brown' demotes positively correlated by PCC; 'color': 'green' demotes negatively correlated by PCC. **Sheet 13** Co-expression network of *E. coli* genes for 3 μg O_3 at 2 hr. 'color': 'brown' demotes positively

correlated by PCC; 'color': 'green' demotes negatively correlated by PCC. **Sheet 14** Co-expression network of *E. coli* genes for 3 µg O_3 at 3 hr. 'color': 'brown' demotes positively correlated by PCC; 'color': 'green' demotes negatively correlated by PCC. **Sheet 15** Co-expression network of *E. coli* genes for 3 µg O_3 control. 'color': 'brown' demotes positively correlated by PCC; 'color': 'green' demotes negatively correlated by PCC. (XLSX 1,055 KB)

Additional file 4: Table S3 Sheet 1 Propensity of *L. monocytogenes* genes selected for 1 µg O_3 network analysis. The 250 most highly expressed and 250 most lowly expressed genes from each treatment [control, 1, 2, and 3 hour (hr)]. Label numbers from 0 to 19 denote genes from most lowly expressed to most highly-expressed. Only those fall into either label 0 or 19 at least in one treatment were selected. Genes differentially expressed based on Pearson Correlation Coefficient (PCC) were shown in columns L-N. **Sheet 2** Propensity of *L. monocytogenes* genes selected for 2 µg O_3 network analysis. The 250 most highly expressed and 250 most lowly expressed genes from each treatment [control, 1, 2 and 3 hour (hr)]. Label numbers from 0 to 19 denote genes from most lowly expressed to most highly expressed. Only those fall into either label 0 or 19 at least in one treatment were selected. Genes differentially expressed based on PCC were shown in columns L-N. **Sheet 3** Propensity of *L. monocytogenes* genes selected for 3 µg O_3 network analysis. The 250 most highly expressed and 250 most lowly expressed genes from each treatment [control, 1, 2 and 3 hour (hr)]. Label numbers from 0 to 19 denote genes from most lowly expressed to most highly expressed. Only those fall into either label 0 or 19 at least in one treatment were selected. Genes differentially expressed based on Pearson Correlation Coefficient were shown in columns L-N. **Sheet 4** Co-expression network of *L. monocytogenes* genes for 1 µg O_3 at 1 hr. 'color': 'brown' demotes positively correlated by PCC; 'color': 'green' demotes

negatively correlated by PCC. **Sheet 5** Co-expression network of *L. monocytogenes* genes for 1 µg O_3 at 2 hr. 'color': 'brown' demotes positively correlated by PCC; 'color': 'green' demotes negatively correlated by PCC. **Sheet 6** Co-expression network of *L. monocytogenes* genes for 1 µg O_3 at 3 hr. 'color': 'brown' demotes positively correlated by PCC; 'color': 'green' demotes negatively correlated by PCC. **Sheet 7** Co-expression network of *L. monocytogenes* genes for 1 µg O_3 control. 'color': 'brown' demotes positively correlated by PCC; 'color': 'green' demotes negatively correlated by PCC. **Sheet 8** Co-expression network of *L. monocytogenes* genes for 2 µg O_3 at 1 hr. 'color': 'brown' demotes positively correlated by PCC; 'color': 'green' demotes negatively correlated by PCC. **Sheet 9** Co-expression network of *L. monocytogenes* genes for 2 µg O_3 at 2 hr. 'color': 'brown' demotes positively correlated by PCC; 'color': 'green' demotes negatively correlated by PCC. **Sheet 10** Co-expression network of *L. monocytogenes* genes for 2 µg O_3 at 3 hr. 'color': 'brown' demotes positively correlated by PCC; 'color': 'green' demotes negatively correlated by PCC. **Sheet 11** Co-expression network of *L. monocytogenes* genes for 2 µg O_3 control. 'color': 'brown' demotes positively correlated by PCC; 'color': 'green' demotes negatively correlated by PCC. **Sheet 12** Co-expression network of *L. monocytogenes* genes for 3 µg O_3 at 1 hr. 'color': 'brown' demotes positively correlated by PCC; 'color': 'green' demotes negatively correlated by PCC. **Sheet 13** Co-expression network of *L. monocytogenes* genes for 3 µg O_3 at 2 hr. 'color': 'brown' demotes positively correlated by PCC; 'color': 'green' demotes negatively correlated by PCC. **Sheet 14** Co-expression network of *L. monocytogenes* genes for 3 µg O_3 at 3 hr. 'color': 'brown' demotes positively correlated by PCC; 'color': 'green' demotes negatively correlated by PCC. **Sheet 15** Co-expression network of *L. monocytogenes* genes for 3 µg O_3 control. 'color': 'brown' demotes positively correlated by PCC; 'color': 'green' demotes negatively correlated by PCC. (XLSX 4,992 KB)

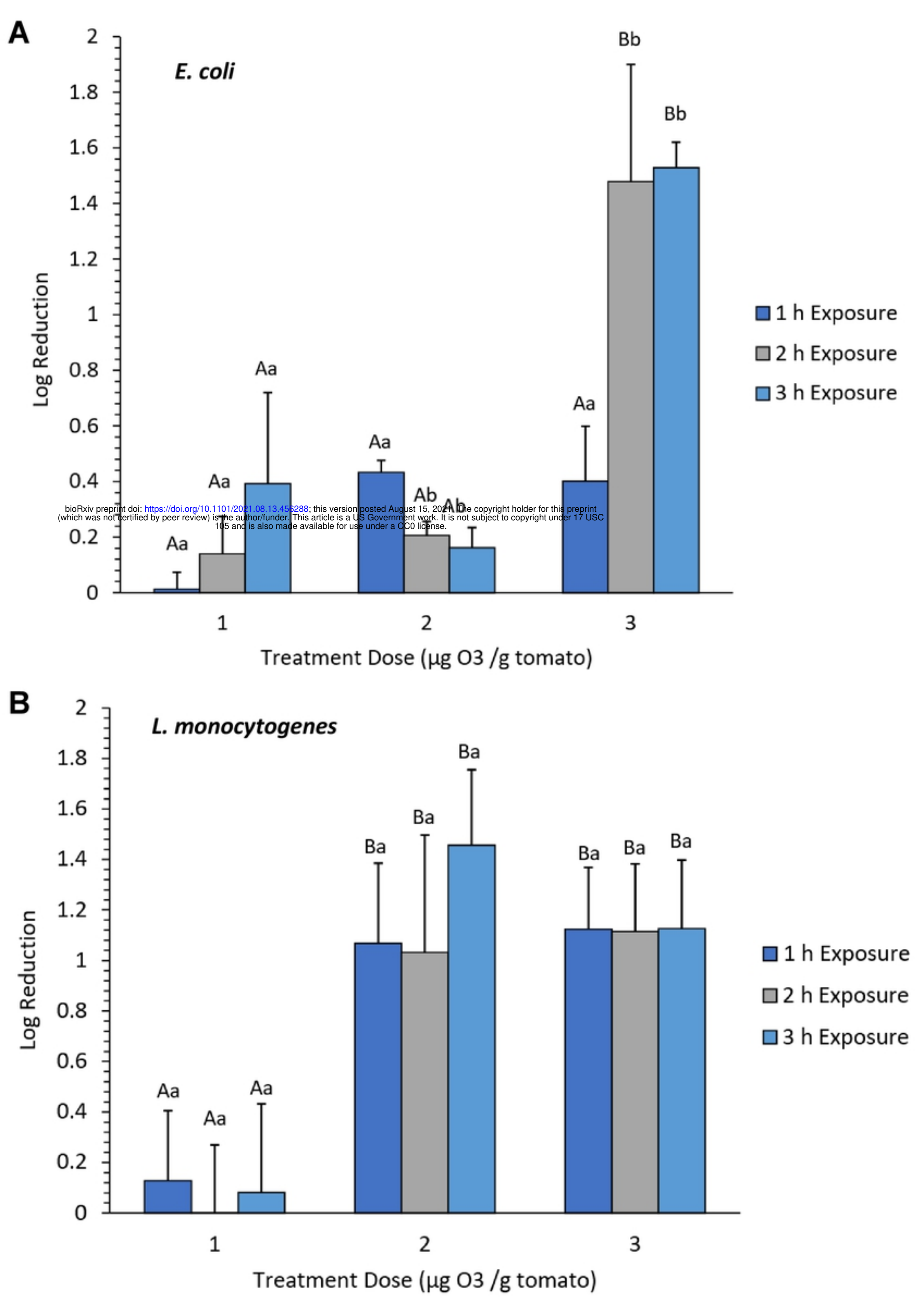

Figure1

A

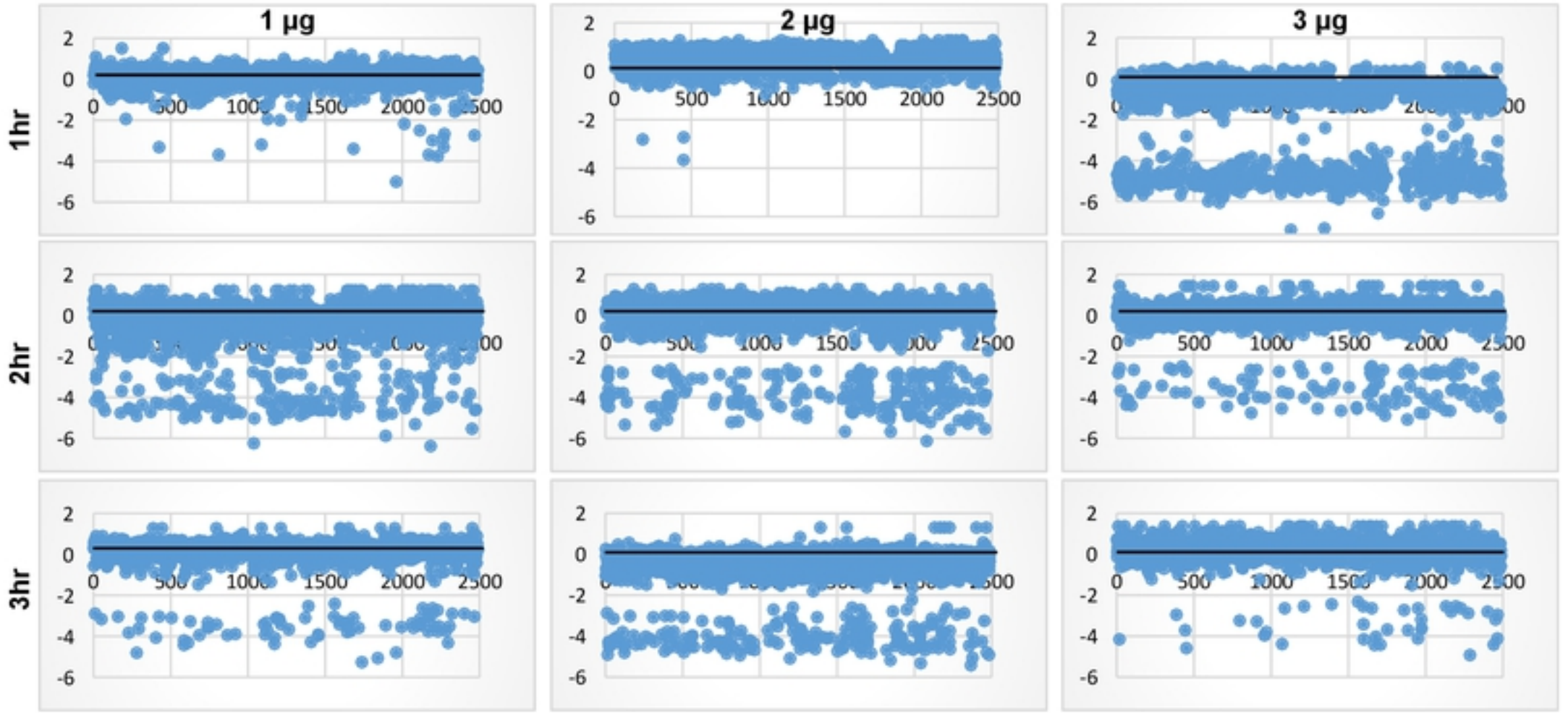

B

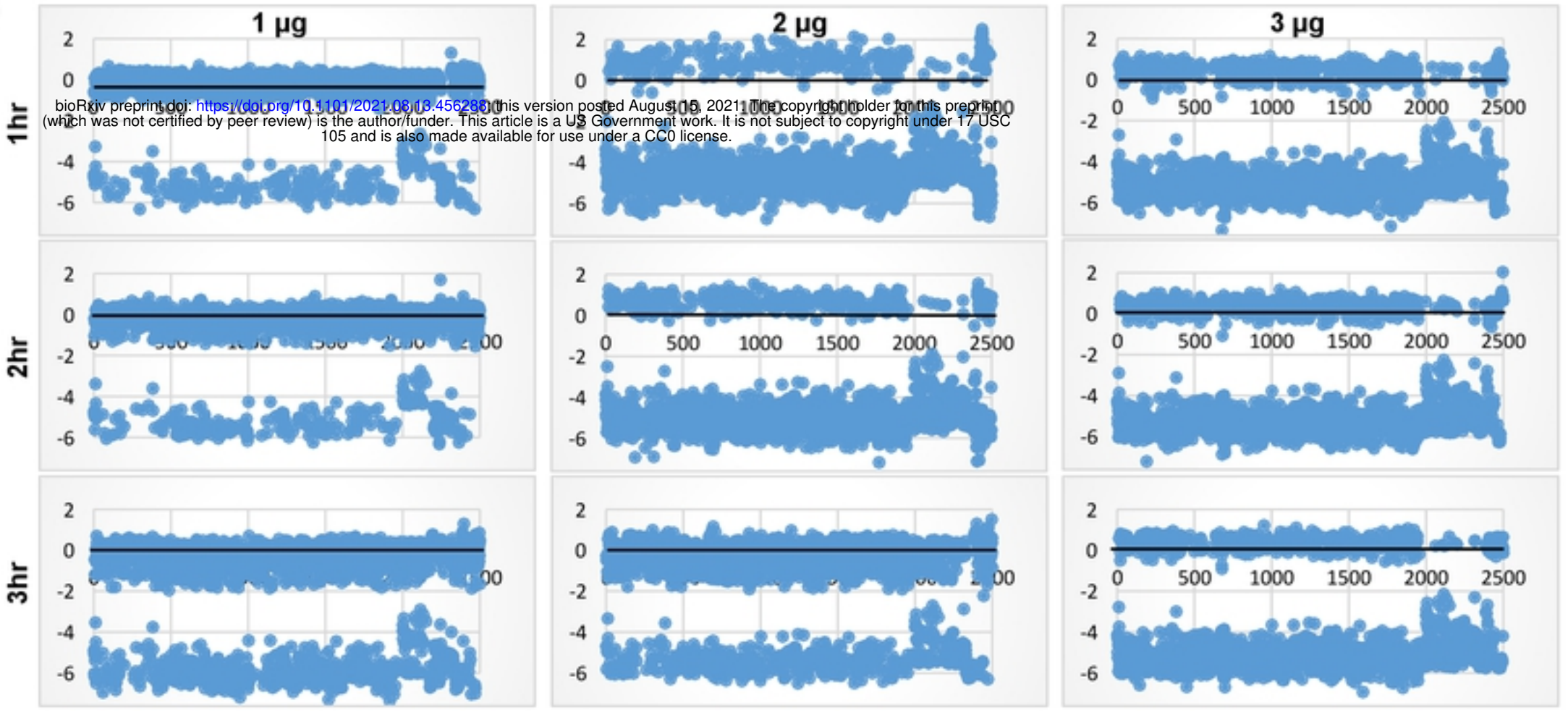

C

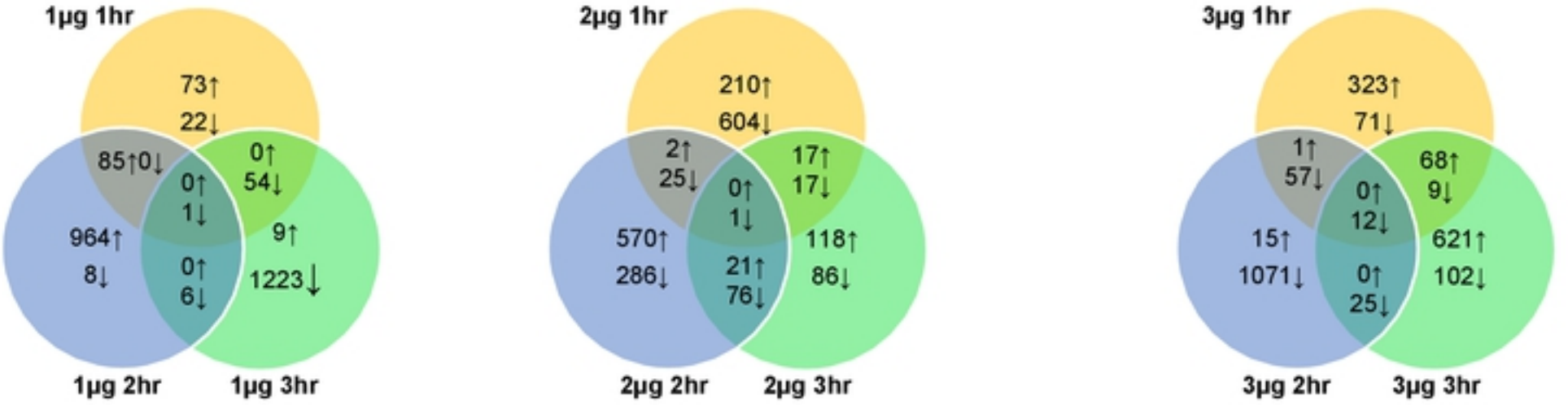

D

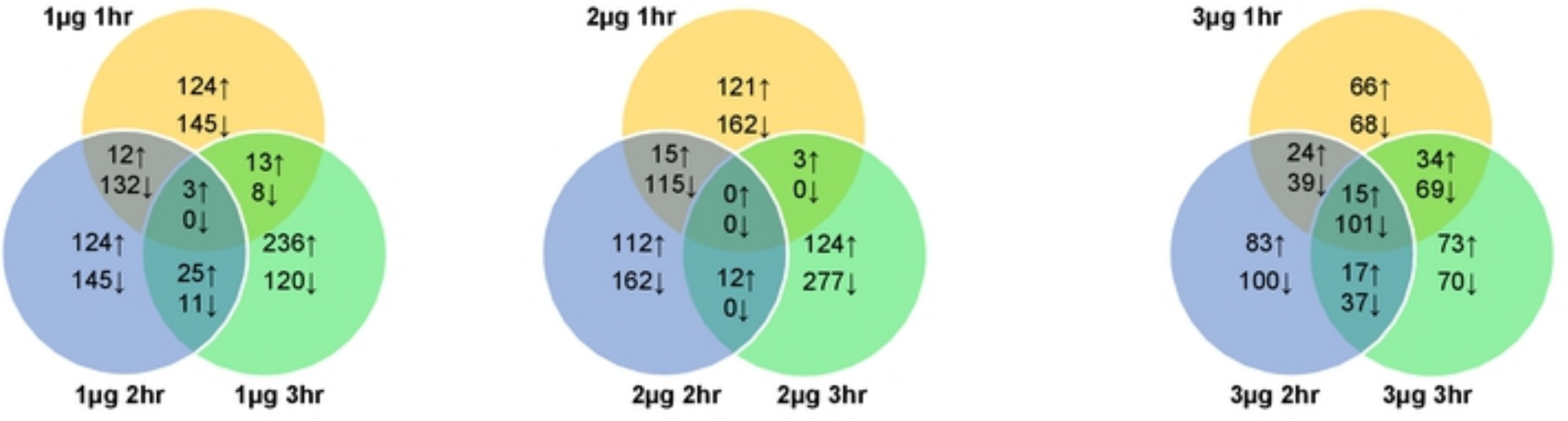

Figure2

A

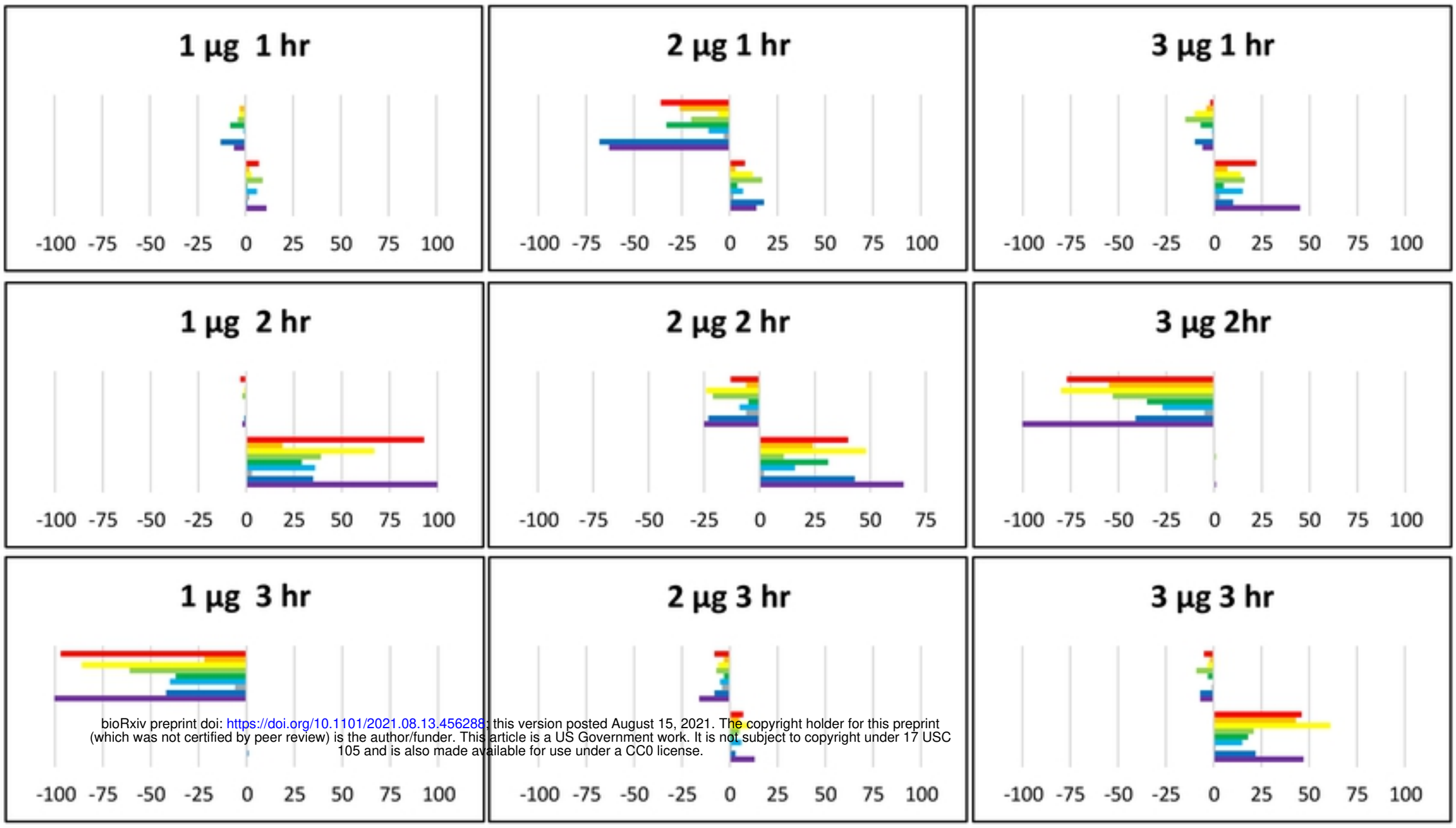

B

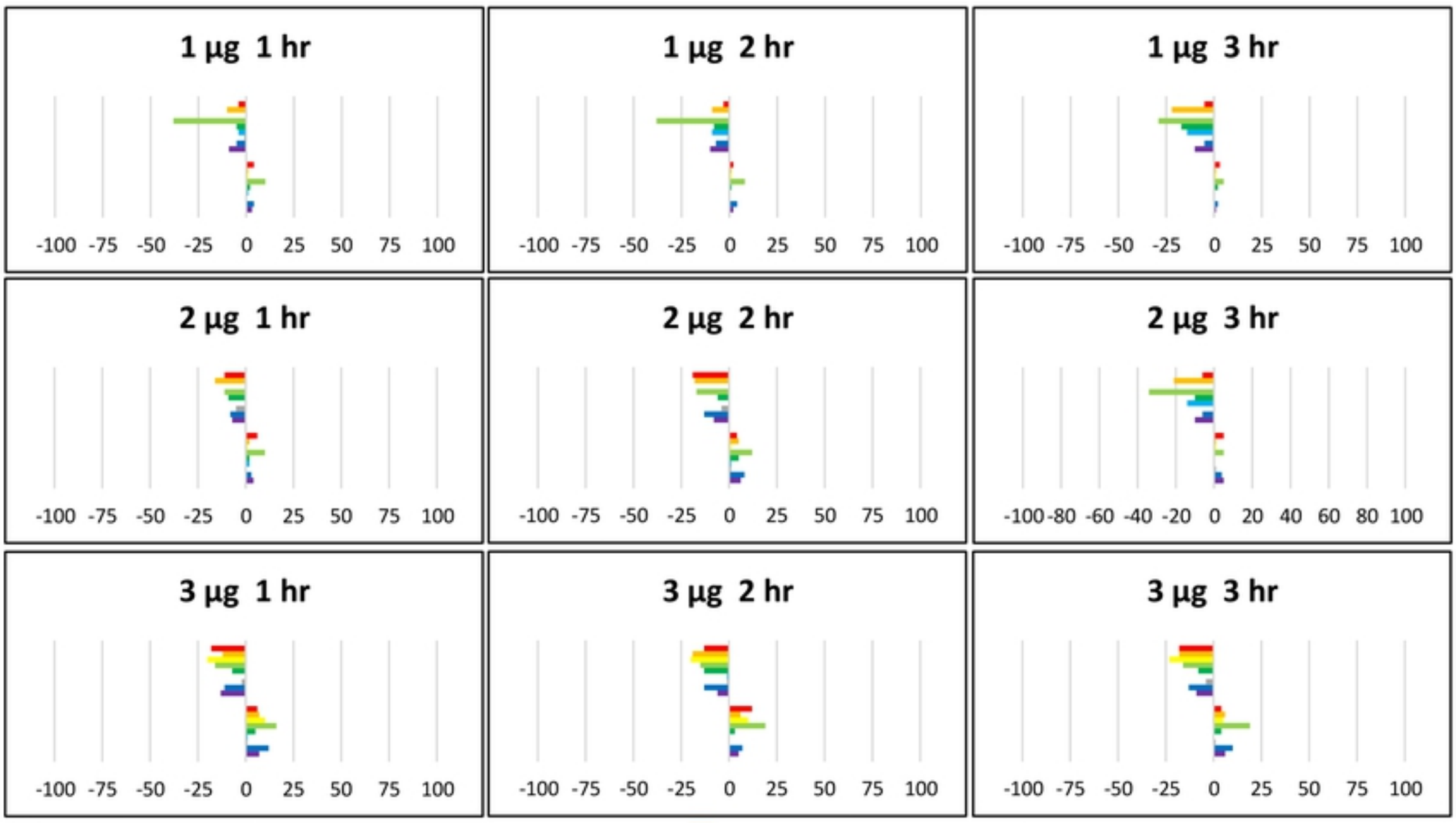

Figure3

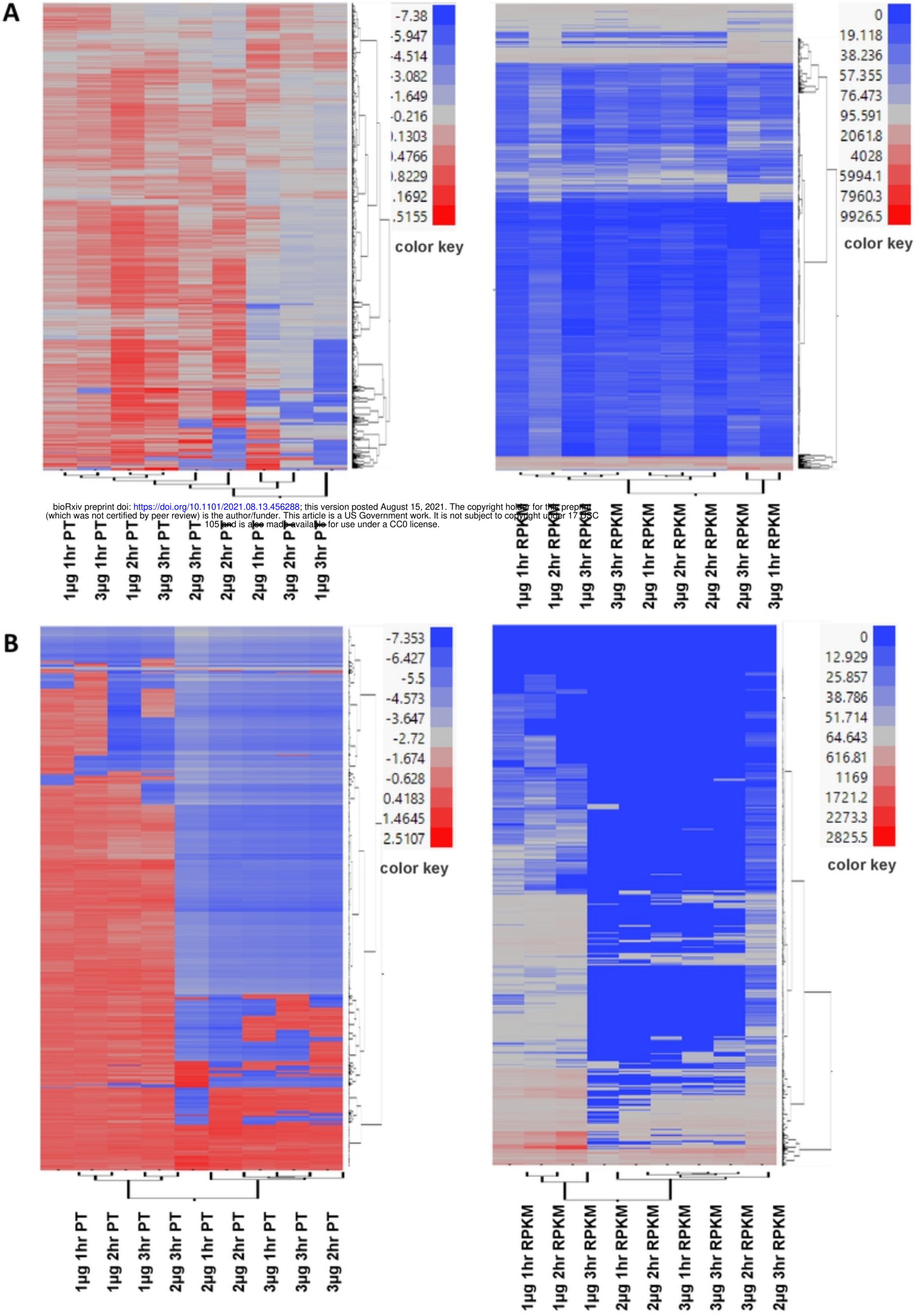

Figure4

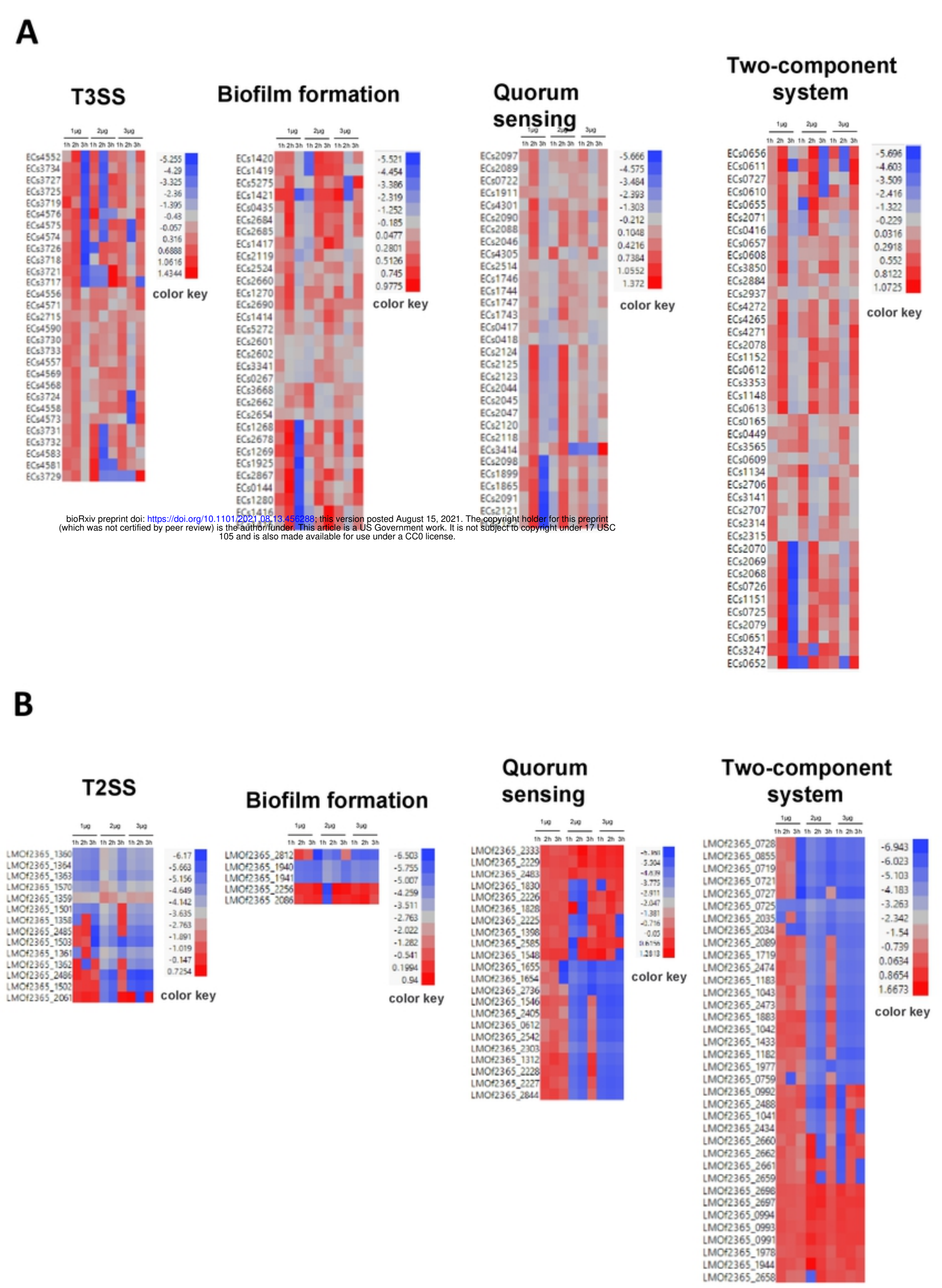

Figure5

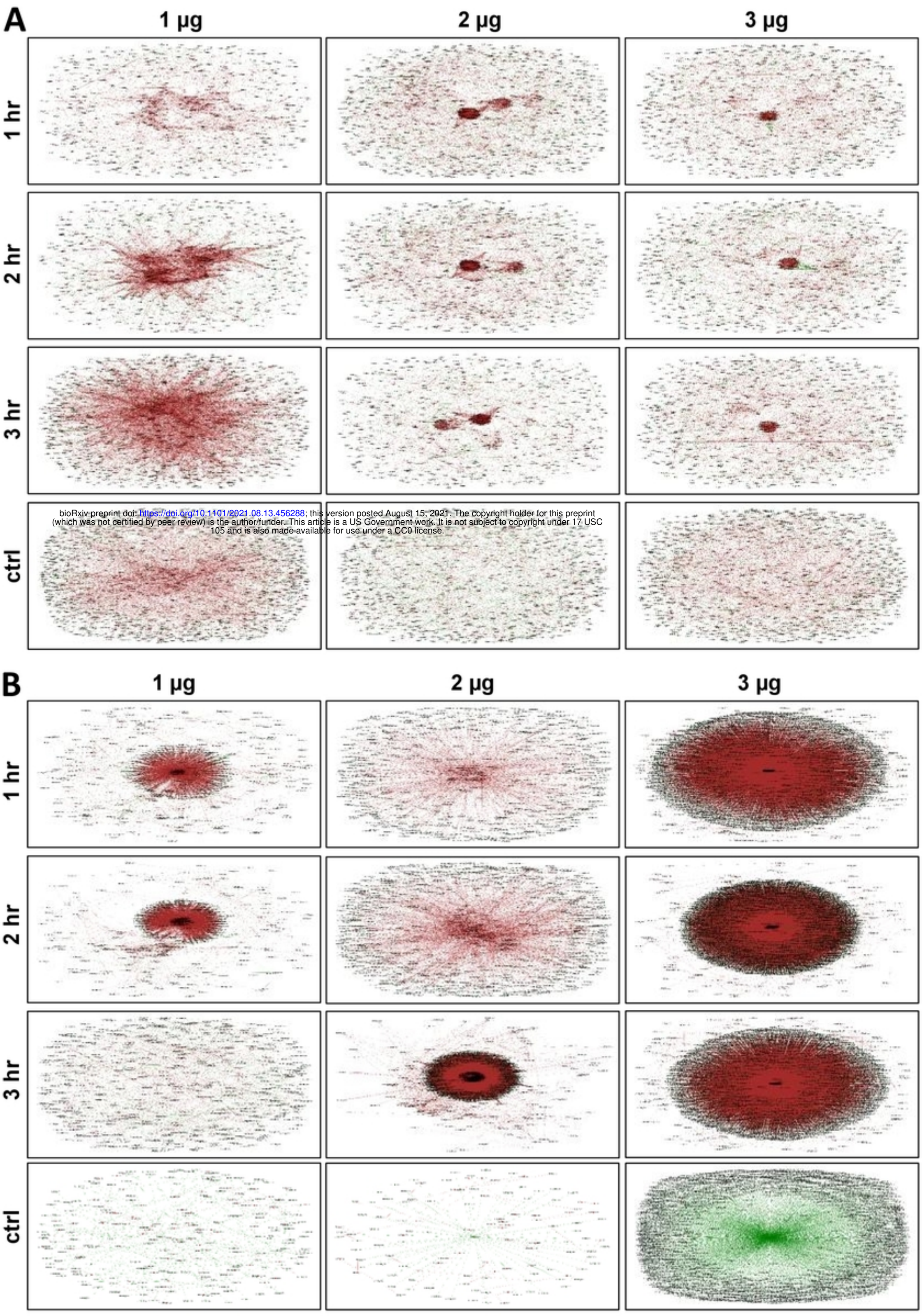

Figure6